Quaternary Science Reviews 346 (2024) 109058

Contents lists available at ScienceDirect

Quaternary Science Reviews

journal homepage: www.elsevier.com/locate/quascirev

Modern land use changes drive shifts in nutrient cycling and diatom assemblages in the Baltic Sea coastal zone: A millennial perspective with a case study from Gamlebyviken, Swedish east coast

Elinor Andrén [a,*], Olena Vinogradova [a], Mikael Lönn [a,b], Simon Belle [c], Martin Dahl [a], Veronica Palm [d,e], Christos Katrantsiotis [f], Anne Birgitte Nielsen [g], Martin Jakobsson [h], Johan Rönnby [d], Thomas Andrén [a]

[a] School of Natural Sciences, Technology and Environmental Studies, Södertörn University, Huddinge, Sweden
[b] Department of Electrical Engineering, Mathematics and Science, University of Gävle, Gävle, Sweden
[c] Department of Aquatic Sciences and Assessment, Swedish University of Agricultural Sciences, Uppsala, Sweden
[d] School of Historical and Contemporary Studies, Södertörn University, Huddinge, Sweden
[e] Västerviks Museum, Västervik, Sweden
[f] Environmental Archaeology Laboratory, Dep. of Historical, Philosophical and Religious Studies, Umeå University, Umeå, Sweden
[g] Department of Geology, Lund University, Lund, Sweden
[h] Department of Geological Sciences, Stockholm University, Stockholm, Sweden

ARTICLE INFO

Handling Editor: Dr P Rioual

Keywords:
Late Holocene
Micropaleontology
Diatoms
Stable isotopes
Organic carbon accumulation rate
Pollen
REVEALS model
LOVE model
Vegetation history
Eutrophication
Bronze Age

ABSTRACT

This study aims to investigate and disentangle the impact of land use and climate variability on the Baltic Sea coastal zone from a millennial perspective. To assess the environmental status of the coastal zone we make use of siliceous microfossils (mainly diatoms), stable nitrogen and carbon isotopes, organic carbon accumulation rates, and lithological changes analyzed in a sediment core collected in Gamlebyviken, Swedish east coast, dated to cover the last 3000 years. Changes in land use and vegetation cover are modelled using pollen stratigraphical data to obtain the percentage coverage of coniferous woodland (*Pinus* and *Picea*), deciduous woodland, wetland (Cyperaceae), grassland (including *Juniperus*) and cropland (cereals) while changes in climatic conditions are assessed through well-documented climatic periods that have occurred in the Baltic Sea region.

The reconstructed regional vegetation cover shows that already 3000 years ago, humans used the landscape for both animal husbandry (grasslands) and farming (cropland), but the impact on the Baltic coastal waters was minor. The diatom accumulation rates were quite high (~3100–2600 cal yr BP) containing taxa indicative of high nutrient conditions/upwelling, and stable carbon isotopes show that the carbon was produced in the basin but did not result in elevated organic carbon accumulation rates. A gradual change to less marine conditions in Gamlebyviken from about 2500 to 1400 cal yr BP can be attributed to the ongoing land uplift which resulted in a more enclosed embayment with only a narrow inlet area today.

The Medieval Climate Anomaly (1000–700 cal yr BP/950–1250 CE) is a time where extensive eutrophication is registered in the open Baltic Sea, but afforestation is recorded between 1000 and 500 cal yr BP and attributed to the expansion of spruce favored by land-use reorganization with a transition from a one-course rotation system to the three-course rotation system fully established in southern Sweden in the 13th century, and only minor environmental change is recorded in the coastal zone.

The Little Ice Age is documented in our data between 400 and 250 cal yr BP/1550–1700 CE as a decrease in regional cropland (cereals) cover, possibly indicating years of poor crop harvest, and changes in the Baltic coastal zone are evidenced as low carbon and diatom accumulation rates, increase in benthic diatom taxa (low turbidity), and high abundance in diatom taxa associated with sea ice indicating a cold climate.

The most significant changes occurred from about 100 cal yr BP/1850 CE up to present, with a maximum regional cover of grassland and cropland (ca. 35%) at the expense of deciduous woodland, and major changes indicative of a highly eutrophic environment recorded in the coastal zone. Organic carbon accumulation rates peaked in 1968 CE at approximately 134 g C m^2 yr^{-1} before subsequently declining to present-day values of 53 g

* Corresponding author.
E-mail address: elinor.andren@sh.se (E. Andrén).

https://doi.org/10.1016/j.quascirev.2024.109058
Received 10 August 2024; Received in revised form 28 October 2024; Accepted 29 October 2024
Available online 18 November 2024

C m^2 yr^{-1}, mirroring a similar trend observed in diatom accumulation rates. The high organic carbon accumulation rate shows that deep unvegetated accumulation bottoms in the coastal Baltic Sea serve as carbon sinks and are worth exploring for their potential in mitigating climate change.

Variation partitioning shows that 26% of the variance in the diatom assemblages is associated with land use changes. The variables grassland, cropland, and stable nitrogen isotopes are accordingly strong predictors of environmental change in the Baltic coastal zone as reflected by the diatom assemblages.

1. Introduction

Deoxygenation of the oceans has been identified as one of the most severe threats to seas globally (Breitburg et al., 2018). Lithological changes serve as a proxy for oxygen status on the seafloor, where laminated sediments (Winterhalter et al., 1981) indicate lack of bioturbation (Jonsson et al., 1990) due to hypoxia/anoxia (Sohlenius et al., 1996; Zillén et al., 2008). Laminated sediments on the seafloor of the open Baltic Sea have been traditionally associated with low oxygen levels induced by warm and dry climatic conditions and elevated salinity (such as during the Holocene thermal maximum approximately 8000–4800 cal yr BP, see also Zillén et al., 2008). However, there is still no consensus regarding the underlying causes of the presence of extensive areas of laminated sediments during the medieval time period.

One hypothesis postulates that the expanding human population in the Baltic Sea catchment area during medieval times extensively employed innovations, such as the steel plow, which by causing increased runoff from the catchment significantly impacted the environmental conditions in the sea, resulting in eutrophication leading to hypoxia in the open Baltic Sea (Zillén et al., 2008). Alternative hypotheses for the development of hypoxic conditions during medieval times incorporate climate variability during the Medieval Climate Anomaly (MCA, 1000-700 cal yr BP/950–1250 CE; Mann et al., 2009). Analysis of diatom assemblages from this time period suggests slightly elevated salinity levels and increased stratification in the Baltic Sea (Andrén et al., 2020), factors that, combined with heightened primary production of cyanobacteria (Kabel et al., 2012) and the proliferation of autumn-blooming diatoms (Andrén et al., 2020), contributed to the exacerbation of benthic hypoxia. Once hypoxia is established in the bottom waters, dissolved inorganic phosphate is released from the sediments as part of internal loading (Conley et al., 2002), thereby becoming available for increased primary production, particularly by cyanobacteria (Vahtera et al., 2007).

Currently, oceanographic models are unable to elucidate the occurrence of medieval hypoxia in the absence of nutrient inputs from land (Schimanke et al., 2012). To explore whether early agricultural practices contributed to hypoxic conditions in the open Baltic Sea, it is essential to examine the impacts on the coastal zone. While numerous studies have examined and dated the onset of contemporary eutrophication in the Baltic Sea coastal zone (e.g., Andrén, 1999; Clarke et al., 2006; Weckström, 2006), there is a shortage of research on the longer millennial time scale. Recent investigations in the Finnish and Swedish archipelagos have revealed minimal environmental changes in the Baltic Sea coastal zone during medieval times and have dated the initiation of eutrophication to the period between 1800 and 1900 CE (Jokinen et al., 2018; Ning et al., 2018; Norbäck Ivarsson et al., 2019).

This paleoecological investigation presents data derived from a long sediment core from Gamlebyviken, a narrow fjord-like estuary situated along the Swedish east coast, with limited present-day connection to the Baltic Sea thus allowing for limited influence of hydrological changes. The primary objective is to investigate the separate influences of land use and climate variability on the Baltic Sea coastal zone within a millennial timeframe. Gamlebyviken was selected as a case study area due to the thousands of prehistoric remains that indicate settlements and activities and therefore had an impact on the regional and local landscapes (Vinogradova et al., 2024), coupled with the estuary's recent susceptibility to and impact from eutrophication (VISS, 2022).

Assessment of the environmental condition of the Baltic Sea coastal zone is conducted through the analysis of siliceous microfossils, predominantly diatoms, stable nitrogen and carbon isotopes, organic carbon accumulation rates, and lithological variations. Modelling of changes in land use and land cover utilizes pollen stratigraphical data extracted from lake sediment cores (Vinogradova et al., 2024), and is complemented by published reconstruction of annual temperature anomalies (Seppä et al., 2009). Multivariate statistical analyses, including variation partitioning, are used to quantify the relative contributions of land use and climate as explanatory variables for environmental changes observed in the Baltic Sea coastal zone over the last 3000 years. Both regional and local modelled land cover data were tested for statistically significant correlations with the response variables (diatom assemblages). Regional land cover was selected for multivariate statistical analyses as it better explained changes recorded in the composition of the diatom assemblages.

2. Historical and regional settings

2.1. Historical land use, and long-term human impact in general

The onset of agriculture in Scandinavia is conventionally associated with the Neolithic period, around 6000 cal yr BP (Welinder, 2011). In south-eastern Sweden, evidence of cultivation emerged at approximately 4600 cal yr BP, evidenced by an increase in pasture and meadow plants alongside the initial appearance of cereals (Berglund, 1991; Berglund et al., 2002; Åkesson et al., 2015). By the Early Bronze Age, approximately 3600 cal yr BP, pollen-based reconstructions of regional vegetation indicate the emergence of an open landscape attributed to the expansion of farms and grazing activities (Åkesson et al., 2015). In southern Sweden, a well-documented expansion of agricultural lands, featuring cultivated and grazed areas, occurred during the Late Bronze Age, at the expense of forests and woodlands (Berglund, 1991; Pedersen and Widgren, 2011). The first millennium BCE witnessed significant agricultural expansion and transformation, attributable in part to climatic shifts during the Late Bronze Age, as well as the adoption of innovative agricultural practices. These practices included the introduction of cattle stalling, the establishment of hay meadows, the implementation of manuring, intensified tillage, and the creation of permanent, stone-cleared fields (Pedersen and Widgren, 2011). Before the late Bronze Age, the predominant cultivated crops in Sweden were millet (*Panicum* sp.) and emmer wheat (*Triticum dicoccum*), but there was a notable shift to hulled barley (*Hordeum vulgare*), possibly in response to the cooling climate conditions.

During the initial centuries of the Common Era, significant technological advancements and shifts in farming practices occurred, notably exemplified by the transition from bronze to iron implements. This transition resulted in alterations to the agrarian landscape, facilitating expanded opportunities for both grazing and grain cultivation (Pedersen and Widgren, 2011).

In the Migration Period during the 5th and 6th centuries CE, extensive reforestation occurred in southern Sweden, and soil erosion was mitigated as many settlements were abandoned, leading to reduced farming and grazing pressures (Berglund, 1991; Åkesson et al., 2015). These changes are evident in both paleoecological and archaeological data from the coastal provinces of south-eastern Sweden (Pedersen and Widgren, 2011), mirroring similar developments that occurred

concurrently across Europe. This phenomenon has been attributed to population decline resulting from infectious diseases and/or a colder climate (Emanuelsson, 2009).

During the Middle Ages in Sweden, spanning approximately from 1000 to 1350 CE, significant alterations in social structure were observed, primarily driven by shifts in landownership, settlement regulations, and the emergence of the open-field system, thereby exerting profound influences on landscape evolution (Myrdal, 2011; Lagerås, 2016). Simultaneously, there was a notable increase in population figures, attributed in part to technological advancements such as the adoption of the wheeled plow (Emanuelsson, 2009), concomitant with a period of climatic warmth recognized as the Medieval Climate Anomaly (Mann et al., 2009).

Around 1350 CE, Scandinavia was harshly impacted by the plague pandemic, causing a marked demographic downturn (Myrdal, 2011). This catastrophic event led to the abandonment of farms and subsequent reforestation of land, particularly in marginal regions previously settled due to heightened population densities and land scarcity, while more fertile territories continued to be cultivated (Lagerås, 2016). Subsequently, a climatic deterioration known as the Little Ice Age (LIA) persisted from roughly 1400 to 1700 CE (Mann et al., 2009), exacerbating crop failures, particularly acute during the 16th and 17th centuries (Myrdal, 2011). Despite these challenges, population growth persisted, driving extensive land clearance activities until approximately 1880 CE (Morell et al., 2011).

From the mid-19th to the mid-20th centuries, water regulation initiatives aimed at reclaiming land for agriculture were implemented across Europe. This involved strategies such as draining through the lowering of lake levels and the ditching of wetlands (Emanuelsson, 2009; Morell et al., 2011). During the 20th century, agriculture underwent a transition towards a system reliant on artificial fertilizers, coupled with advancements in plant breeding and the adoption of more efficient machinery. These developments resulted in higher yields per unit area, as well as lower demand for grazing land and hay meadows, leading to the overgrowth or transformation of less fertile parts of the landscape into spruce plantations characterized by low biodiversity (Emanuelsson, 2009).

2.2. Historical land use in the study area

In the study area surrounding the Gamlebyviken, fossil pollen-based palaeoecological reconstructions and archaeological data testify continuous human activity during the last 3000 years with interchanging intervals of increase in agriculture and landscape openness, and periods of reforestation (Vinogradova et al., 2024). Locally, significant landscape openness during the Bronze Age and Early Iron Age (3100-2000 cal yr BP) is supported by archaeological mapping reflecting substantial human influence on the landscape surrounding Gamlebyviken during the Bronze Age. The regional pollen-based indications of anthropogenic activity remain relatively low during the Bronze Age and larger part of the Iron Age (until 1650 cal yr BP). Strong increase in landscape openness and crop cultivation both regionally and locally is reconstructed during the Late Iron Age until the beginning of the Middle Ages (between 1650 and 1000 cal yr BP). The following period of increase of woodland cover during the Middle Ages, usually associated in Sweden with increased agricultural activity, is due to the expansion of spruce (*Picea*), that occurred both regionally and locally. During the modern time (450 cal yr BP – present), pronounced increase in vegetation openness with expansion of grassland and high cover of cropland is reconstructed locally. Regional plant cover also reflects increase in grassland and cropland but remains woodland-dominated.

2.3. The Baltic Sea environment

The Baltic Sea is today one of the world's most impacted seas, suffering from severe environmental problems caused by human activities in the densely populated catchment area, and during the last decades also an increased impact from climate change (Meier et al., 2022). The environmental problems of the Baltic Sea are enhanced by its geography with its northerly location and semi-enclosed configuration, with only limited exchange of marine waters, which create stratified water masses (Snoeijs-Leijonmalm and Andrén, 2017). The surface water salinity is low and has a gradient from almost zero in the northern parts with large freshwater runoff to about 10 at the thresholds (the Danish Sounds and Öresund) in the south (Leppäranta and Myrberg, 2009). The deep waters of the Baltic Proper are periodically replenished by episodic inflows of substantial volumes of highly saline water (17–25) from the North Sea, crossing various thresholds (HELCOM, 2007). This process establishes a salinity gradient also in the deep waters, with salinity levels approximately 6.5 in the northern part, around 12 in the central Baltic Proper, and about 15 in the south near the straits (Snoeijs-Leijonmalm and Andrén, 2017). The residence time of water is about 30–40 years which exacerbates the contamination with toxic compounds as well as nutrient enrichment causing eutrophication and widespread hypoxia (Snoeijs-Leijonmalm and Andrén, 2017). The coastal areas of the Baltic Sea are increasingly affected by frequent hypoxia and host a significant number of the world's known hypoxic sites (Conley et al., 2011). Over the past century, the extent of hypoxia in the open sea has expanded tenfold, now encompassing an area of nearly 70,000 km^2 (Carstensen and Conley, 2019).

Ongoing climate change results in warming, and at northern latitudes the rate of warming surpasses the global average. Consequently, the Baltic Sea region has experienced a more pronounced annual mean temperature anomaly over the past century compared to the global mean (Meier et al., 2022). This heightened sensitivity to climate fluctuations renders the Baltic Sea region an ideal location for investigating long-term climate effects. The high-resolution soft sediments found in Gamlebyviken, characterized by an annual sedimentation rate of up to 10 mm yr-1, provide an exceptional historical archive favorable to paleoecological studies.

The Baltic Sea is a geologically young sea, influenced by the glacial and postglacial history of the area affecting isostacy and eustacy (Andrén et al., 2011). The present geographical configuration of the basin emerged when the world ocean sea level rose and inundated the thresholds in the south and marine waters started to enter the basin about 9800 to 8000 years ago (Andrén et al. 2000a, 2000b, 2011). During the following stage, called the Littorina Sea, more marine conditions prevailed and salinity stratification together with the warmer conditions during the coinciding Holocene Thermal Maximum resulted in large areas of hypoxia and cyanobacterial blooms in the open basin (Bianchi et al., 2000; Zillén et al., 2008).

2.4. Study site

Gamlebyviken is a ca 20 km long and 1–2.5 km wide fjord-like estuary situated in south-eastern Sweden with a 5-m deep sill separating it from the Baltic Sea (Fig. 1B). The estuary consists of two basins separated by a shallow area about 16 m deep; an inner basin of 9.6 km^2 and a maximum water depth of 57 m and the outer basin covering an area of 17.1 km^2 and a maximum water depth of 25 m (VISS, 2022; Eniro På sjön 2022). There are several small streams discharging in the inner basin of Gamlebyviken of which Dynestadsån, Gamlebyån, and Almviksån are the main ones (Fig. 1B). The salinity in Gamlebyviken is about 5.5 in the surface and 6 in the bottom waters, compared to about 7 in the surface water in the Baltic Sea outside the sill (VISS, 2022).

The estuary is today significantly impacted by point sources, e.g. two sewage treatment plants, but also by diffuse sources such as urban areas, agriculture, forestry, and atmospheric deposition. The ecological status of the inner Gamlebyviken is considered poor to moderate when using biological and chemical quality indicators such as Secchi depth, nutrients, and chlorophyll-a from the three monitoring stations (VISS, 2022). The estuary regularly displays low oxygen concentrations, hypoxia (O_2

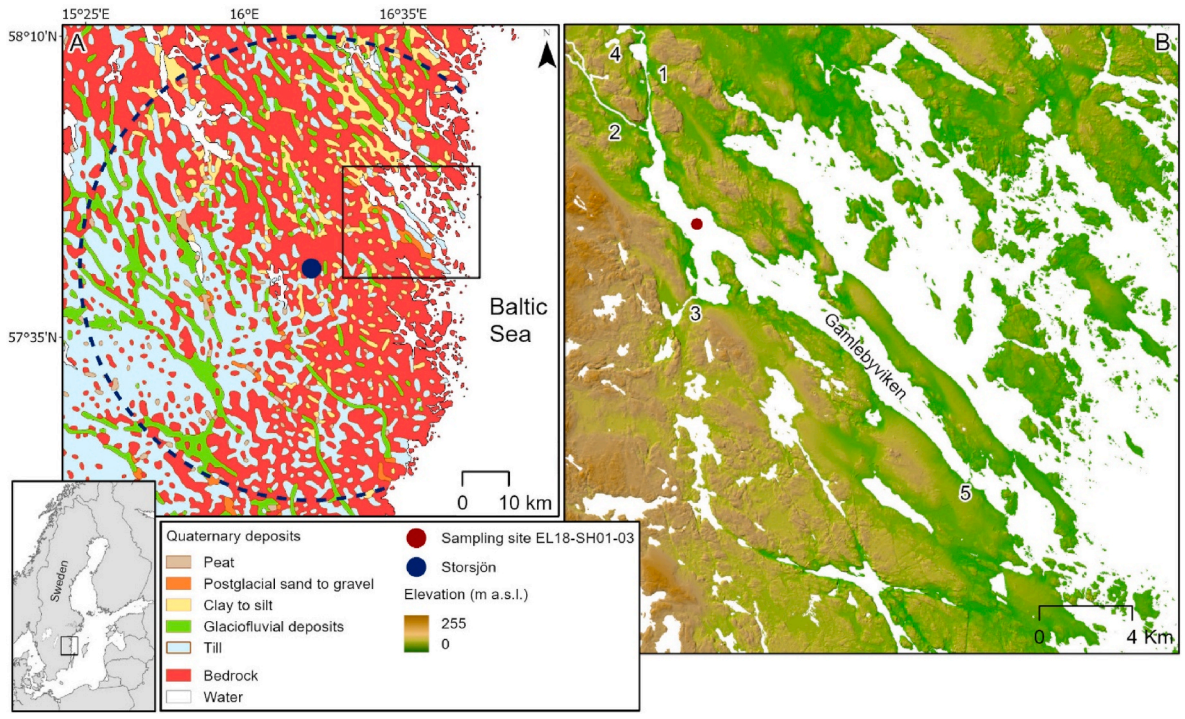

Fig. 1. Map of the Gamlebyviken study area and its location in Scandinavia. A. The Quaternary deposits and the location of Lake Storsjön which was used to reconstruct regional changes in landscape openness in the study region, within an area of a 50 km radius (the dashed circle). B. Elevation map and the location of the sampling site EL18-SH01-03 (N 57°51.690′, E 16°26.913′) in the Gamlebyviken estuary. Streams discharging in the inner part of Gamlebyviken are 1 Dynestadsån, 2 Gamlebyån and 3 Almviksån. Number 4 indicates the location of the small Lake Lillsjön, which is utilized for local vegetation reconstruction. The narrow inlet to the estuary, marked as number 5, is situated in the town of Västervik.

< 2 mg L^{-1}), at the sea floor in the summer months.

The Quaternary deposits in the area surrounding the inner parts of Gamlebyviken consist of glacial and post-glacial clays in the valleys and till combined with bedrock outcrops on higher elevations (Fig. 1A; SGU, 2022). The present land uplift in the area is about 2.5 mm per year (Svantesson, 1999).

The study region belongs to the hemiboreal zone (Ahti et al., 1968) dominated by pine or spruce forests, but on the Swedish east coast deciduous trees are widespread (Sjörs, 1999). The climate is maritime with an annual mean temperature of ca 8 °C and a mean annual precipitation of about 600 mm (mean of the years 2002–2021; SMHI, 2022).

3. Material and methods

3.1. Collection and handling of sediment cores

To select the most appropriate coring site a pre-site survey was performed in August 2018 from R/V Electra af Askö using multibeam echo sounding complemented with sub-bottom profiling. Four sites along a NW-SE transect in the deepest inner part of Gamlebyviken, plus two additional sites closer to the northern shore, were chosen based on the presite survey. Off-shore coring was performed by a combination of a 6-m long piston corer supplemented with a 1-m gravity corer to collect the topmost soft sediment. The piston cores were cut into 1.5 m sections, sealed with end caps, and put in a cold container together with the gravity cores onboard the ship for later transport to the laboratory. The sediments of all piston cores were cut in halves lengthwise, opened and lithologically described in laboratory. Color was determined using the Munsell soil-color charts (Munsell Soil Color Book, 2009). The short gravity cores were pushed out of their tube from the bottom, sliced in 1 cm thick slices at the top and put in zip-lock bags. A parallel short core was pushed out using a piston to describe the lithology of the sediment. Station EL18-SH01-03 (N 57°51.690′, E 16°26.913′) situated in the deepest part at 55 m water depth contained the sediment sequence with the highest resolution, i.e. the highest sediment accumulation rate, and was selected as the master station and subsequently used for all further analyses in this study (Fig. 1B).

3.2. Geochemistry

Every 10 cm were analyzed throughout the core for carbon and nitrogen stable isotopes, $\delta^{13}C_{OM}$ and $\delta^{15}N_{OM}$, respectively. Sediment samples were dried at 60 °C for 72 h, ground, and about 3 mg of dried sediments were transferred to silver capsules, and carbonate removal was done using small additions (50 μL) of HCl 1 M. Carbonate-free sediment samples were then introduced in tin capsules and analyzed using an Isotope Ratio Mass Spectrometer interfaced with an Elemental Analyzer (EA-IRMS) at the Stable Isotope Laboratory, Swedish University of Agricultural Sciences in Umeå, Sweden. Results were expressed as the delta notation with Vienna Pee Dee Belemnite and atmospheric nitrogen as standards: $\delta^{13}C$ or $\delta^{15}N$ (‰) = [(Rsample/Rstandard) – 1] x 1000; where $R = {}^{13}C/{}^{12}C$ or ${}^{15}N/{}^{14}N$. Sample measurement replications from internal standards (wheat and mays flour) produced analytical errors (1σ) of ±0.15‰ for both $\delta^{13}C_{OM}$ and $\delta^{15}N_{OM}$ values (n = 24).

Organic carbon content was analyzed in the sediment every to every other cm in the top 77 cm and thereafter every 10th cm using loss-on-ignition (LOI) in 550 °C (Dean, 1974). Samples of about 1 cm^3 of wet sediment were put in crucibles of known weight and dried at 105 °C overnight and then put in a desiccator to cool down. The sediment dry weights (DW) were obtained, and crucibles were placed in a furnace set for 550 °C. The furnace was slowly heated, with about 30 min to reach the set temperature, and samples thereafter burnt for 75 min. Samples were cooled in a desiccator and weighted. The percentages of dry weight of organic matter could thereafter be calculated. Dry mass accumulation rates (DMAR, g $cm^{-2}yr^{-1}$) were calculated by multiplying the sedimentation rate (cm yr^{-1}) by the sediment dry bulk density (ρ gcm^{-3}),

and subsequently multiplied with organic matter to derive organic matter accumulation rates. Organic matter from LOI measurements are correlated with organic carbon content. To convert organic matter accumulation rates to organic carbon accumulation rates (g C $m^{-2}yr^{-1}$) we used the correction factor of 0.385, valid for coastal sediments from the north-western Baltic Proper (Jonsson, 2003).

3.3. Construction of splice record and chronology

The long piston and short gravity cores were correlated to each other by wiggle-matching the plotted graphs of organic matter and stable carbon and nitrogen isotope records to construct the splice core record.

The splice core chronology is based on accelerator mass spectrometry (AMS) radiocarbon dating for the older part supplemented by ^{210}Pb and ^{137}Cs for the younger part. Macrofossils samples extracted from the sediments were submitted to the Tandem Laboratory at Uppsala University, Sweden for AMS radiocarbon dating. Radiocarbon dates were converted to calibrated years before present (cal yr BP) using Calib rev. 8.2 (Stuvier and Reimer, 1993) and the age-depth model was constructed using the Bayesian statistics modeling R-module BACON version 2.5.8 (Blaauw et al., 2022; Blaauw and Christen, 2011) and the IntCal20 calibration data set (Reimer et al., 2020) in the software R.4.2.2 (R Core Team, 2022). Two samples, Ua-62009 and Ua-62015, were identified as being of marine origin based on their δ^{13}C values. Therefore, the Marine20 calibration dataset (Heaton et al., 2020) was used for these samples, with an (R) value of 295 ± 50 as reported in the Marine Reservoir Correction Database (http://calib.org/marine/), Map No. 1710 (Lougheed et al., 2013). The age-depth models are based on linear interpolation between the midpoints of 1-sigma calibrated age ranges. Weighted average estimates of calendar ages were obtained for every depth.

St. Croix Watershed Research Station, Science Museum of Minnesota, USA, analyzed the short gravity core for the activities of ^{210}Pb and ^{137}Cs using gamma spectrometry. The measurements were carried out on a Canberra ultralow background Ge-well-detector. The Constant Rate of Supply (CRS) method was applied for the cores using the modified method by Appleby (2001). In addition to the ^{137}Cs signal deriving from the Chernobyl accident in 1986 CE we also included the increase in ^{137}Cs-curve attributed to the atmospheric testing of nuclear weapons dated to ca 1960 CE in the age determination. The lower parts of the cores were dated by a linear regression assuming constant sediment accumulation.

3.4. Siliceous microfossils

Sediments for analyses of siliceous microfossils were prepared according to methods described in Battarbee (1986) using 30% hydroperoxide to oxidize organic matter and several decanting steps to clean the sediment from clay particles. To measure the concentration (absolute abundance) of siliceous microfossils the microsphere method was used (Battarbee and Kneen, 1982). By counting microspheres with a known concentration, the absolute abundance, in number of valves per g DW could be calculated as: number of microspheres introduced multiplied with the number of microfossils counted, divided by the number of microspheres counted and the sediment dry weight. 0.2–0.4 g of freeze-dried sediment was weighed and 1 mL stock solution of microspheres with a concentration of 5.56×10^6 per mL was added in the last step before preparation of the diatom slurry on cover slides which after drying at room temperature were mounted in Naphrax™. The absolute abundance of diatoms was multiplied by DMAR to obtain the accumulation rates.

Counting of microfossils (mainly diatoms) was carried out with a light microscope Olympus BX51 using Nomarski differential interference contrast at a magnification of 1000× and oil immersion. *Chaetoceros* spp. were not identified to species level and include both vegetative cells and resting spores. To record also the less common diatom taxa a minimum of 300 valves were counted in every analyzed sediment layer excluding mass-occurring taxa such as *Chaetoceros* spp. and *Skeletonema marinoi*, even though all valves were counted and included in the basic sum. The diatoms were classified into life forms (planktonic(free living in the water), benthic (attached or motile on the sea bottom), epiphytic (part of the benthics attached to plants/algae), and unclassified) and salinity preferences (marine (including both marine-brackish and brackish-marine affinity), brackish, brackish-freshwater, freshwater, unclassified salinity, and sea ice). When calculating the planktonic/benthic diatom ratio the epiphytes were included as a part of the benthic assemblages. The following species have been classified as sea ice diatoms (sympagic) living in and on sea ice: *Fragilariopsis cylindrus, Melosira arctica,* and *Pauliella taeniata* (Meiners et al., 2002; Thomas et al., 2017). Floras used for species identifications and classification of environmental affinity were Hasle and Syvertsen (1997), Krammer and Lange-Bertalot (1986–1991), Snoeijs et al. (1993–1998) and Witkowski et al. (2000), and taxonomic names are updated according to AlgaeBase (Guiry and Guiry, 2024; www.algaebase.org/).

A stratigraphically constrained cluster analysis was carried out on a subset of the diatom data (i.e. only including species with relative abundance data >2%) using CONISS in the Tilia 2.1.1 software (Grimm, 1987). Detrended Correspondence Analysis (DCA) was used on the whole diatom data set to record the overall compositional change in the diatom assemblages using the package rioja and vegan in R 4.2.2 (Juggins, 2015; Oksanen et al., 2022). To calculate diatom species richness a rarefaction analysis was performed on the same diatom data set using the vegan package (Birks and Line, 1992; Oksanen et al., 2022).

3.5. Paleogeographical maps

Paleogeographical maps illustrate the land-sea configuration of a specific area over time. These maps were created using ArcGIS Pro (v. 3.1.1) and were based on the shoreline displacement curve from Katrantsiotis et al. (2024) for two time periods (i.e., 3000 and 1300 cal yr BP). The calculations for the current shoreline level were based on a digital elevation model (derived from LiDAR data from the Swedish National Land Survey with an altitude resolution of 0.1 m).

3.6. Quantitative estimation of regional and local land cover

Estimation of land use and resulting land cover changes as a component for statistical analysis was performed using the Landscape Reconstruction Algorithm (LRA) with its two submodels, REVEALS (Regional Estimates of Vegetation Abundance from Large Sites; Sugita, 2007a) and LOVE (LOcal Vegetation Estimates; Sugita, 2007b) using parameter settings presented in Vinogradova et al. (2024). Pollen data from the large lake Storsjön (Ning et al., 2018; Åkesson, 2013) and the small lake Lillsjön (Vinogradova et al., 2024) were used for regional and local land cover reconstructions, respectively. Storsjön is situated approximately 29 km west from the coast and 21 km SSW from the Gamlebyviken (Fig. 1A), i.e. within the 50 km-area around a large lake covered by regional reconstructions (Sugita, 2007a). The inner part of Gamlebyviken (Dynestadsån, no. 1 in Fig. 1B) falls within the 2 km radius of the small lake (Lillsjön, no 4 in Fig. 1B), the area within which the local vegetation reconstruction is applicable (Vinogradova et al., 2024). Thus, it was possible to reconstruct landscape changes at both the regional and local scales in the Gamlebyviken area. Compared to Vinogradova et al. (2024) the LRA was run with increased resolution of 16 time windows (TW), which was a balance to maximize both time resolution (necessary for informative statistical analysis) and pollen counts per time window (necessary for reliable modelling). The span of the time windows is the date of coring - 100 cal yr BP (1 TW), 150 yr between 100 and 1450 cal yr BP (9 TW), 200 yr between 1450 and 2250 cal yr BP (4 TW), 400 yr from 2250 to 2650 cal yr BP (1 TW) and 430 yr from 2650 to 3080 cal yr BP (1 TW). The 28 taxa included in the LRA

modelling (Table S1, supplementary material) were grouped into five land cover types (modified after Mazier et al., 2015) which were used in the statistical analyses: coniferous woodland (*Pinus* and *Picea*), deciduous woodland, wetland (Cyperaceae), grassland (including *Juniperus*), and cropland (cereals).

3.7. Multivariate statistics

Calculations were performed in the statistical environment R 4.2.2 (R core team 2022). The resolution of the used variables (land cover types, temperature, geochemistry) are different from the diatom data, therefore we used Generalized Additive Models (GAMs) to smooth the explanatory variables and then used predicted values from these models at the years covered by the diatom data.

For an overview of the association of the explanatory variables with the diatom assemblage composition, we performed a Principal Component Analysis (PCA). Each explanatory variable was regressed onto the ordination to show the direction and evaluate the significance of their association using the function "envfit" in the R-package "vegan" (Oksanen et al., 2022).

In the PCA the separate effects of the explanatory variables taking the other variables into account cannot be evaluated. The explanatory variables are more or less correlated and to sort out their individual effects we took two approaches using Redundancy Analysis (RDA). In this analysis, all five land cover types cannot be used because they add up to 100% (the fifth one is fully described by the four others) so we chose the two land cover types assumed to be most clearly associated with human impact, grassland and cropland. We used the "anova by margin" function in the RDA model, where all variables are tested for significance after the effects of other variables are removed. This approach identifies the variable with the largest unique influence.

To compare the size of the effect of time, temperature, nitrogen isotopes, and land use we performed variance partitioning using the function "varpart" in "vegan". Only four variables are allowed in "varpart" so grassland and cropland together were chosen to represent land use. The cluster analysis performed using the R-package "rioja" revealed four diatom assemblage zones in the sequence. The first and last zones were too small for variance partitioning so we divided the data into one older part, zones 1 and 2 and one younger part, zones 3 and 4.

To find the explanatory variables that had a significant effect on explaining changes in the diatom species and avoid problems with multiple testing we used "Random Forests" as implemented in the R-package "Boruta" (Kursa and Rudnicki, 2010) using the recommended significance level 0.01. For each explanatory variable, we obtained a list of which diatoms are important. Since the "Random Forests" method builds on regression trees the diatoms are evaluated in interaction with other diatoms. To get information on the direction of the associations between diatoms and variables we made a correlation table but only interpreted the correlations that were important according to the "Random Forests" output.

4. Results

4.1. Age-depth modelling and chronology

It was possible to construct an age-depth model for the splice core covering the last ca. 3500 years (Fig. 2). Eleven levels were radiocarbon dated and nine of these were used in the age model (Table 1). The resulting sediment accumulation rate is stable around ca. 1.5 mm/yr with only small variations from the bottom of the core until the upper ca. 50 cm. From this core-depth, accumulation increases to around 10 mm/yr.

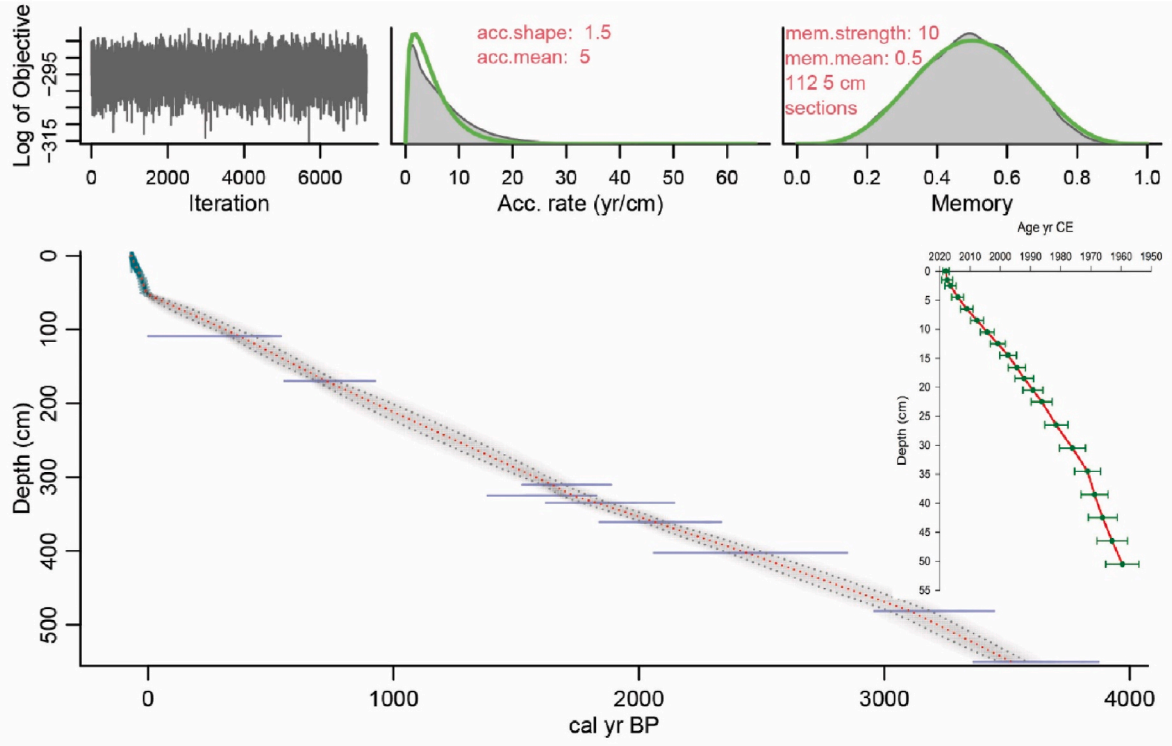

Fig. 2. Gamlebyviken estuary: age-depth model for the splice core from site EL18-SH01-03 using BACON ver. 2.5.8 (Blaauw and Christen, 2011; Blaauw et al., 2022). The age model covers the last 3500 years and uses ^{210}Pb and ^{137}Cs in the youngest part (<100 years) and nine radiocarbon dates calibrated using the IntCal20 dataset (Reimer et al., 2020) and Marine20 (Heaton et al., 2020) in the older part. Upper panels left depict the Markov Chain Monte Carlo iterations, the prior (green curves) and posterior (grey histograms) distributions for the accumulation rate (middle panel) and memory (right panel). The bottom panel shows the calibrated ^{14}C dates and the red stippled line corresponds to the model's best fit based on the mean age for each depth and the grey stippled lines delimit 95% confidence intervals. The right panel show the age-depth model for the youngest part of the sediment core derived from ^{210}Pb and ^{137}Cs (years CE).

Table 1
Gamlebyviken esturary: core EL18-SH01-03-PC01 uncalibrated and calibrated radiocarbon ages (2σ). Calibration was performed using Calib rev. 8 (Stuiver and Reimer, 1993), Intcal20 calibration datasets (Reimer et al., 2020) and Marine20 (Heaton et al., 2020). (*) = Not enough material for analysis. *Italics* indicate samples not used in the age-depth model.

Lab code	Depth in core (cm b.s.f.)	Depth in splice (cm b.s.f.)	Dated material	$\delta^{13}C$ (‰)	^{14}C age (yr BP)	Error (cal yrs)	Mean calibrated age (min – max) (cal yr BP)
Ua-62008	31–33	109	Plant remnants	−28.8	368	35	407 (315–499)
Ua-62009	92–94	170	Fish skeleton	−18.3	797	45	726 (668–784)
Ua-62010	232.5–234	310.25	Plant remnants	−27.4	1788	35	1659 (1571–1746)
Ua-62011	247–248.5	324.75	Plant remnants, reed	−26.2	1714	41	1619 (1533–1704)
Ua-62012	257–258	334.5	Plant remnants	−25.1	1948	42	1866 (1745–1987)
Ua-62013	283–285	361	Plant remnants, seeds and charcoal	−24.0	2111	34	2123 (1953–2293)
Ua-62014	324.5–326.5	402.5	Plant remnants and charcoal	−27.1	2890	42	2497 (2319–2574)
Ua-62015	403.5–405	481.25	Plant remnants and seeds	−17.6	3038	38	3221 (3082–3360)
Ua-62016	*472.5–473.5*	*517*	*Seed*	*(*)*	*3772*	*76*	*4168 (3929–4407)*
Ua-62017	472.5–473.5	550	Plant remnants	−23.0	3347	45	3575 (3460–3690)
Ua-62018	*515–517*	*593*	*Plant remnant*	*(*)*	*3514*	*167*	*3817 (3392–4242)*

4.2. Lithology, organic matter, and organic carbon accumulation rates

The lithology of sediment station EL18-SH01-03 consists of mud (clay-gyttja) with sulphide banding and laminations throughout (Table S2, supplementary material). Some sequences were completely black which prevented distinguishing structures but they became visible when oxidized. Organic matter shows the highest content in the oldest part between 3100 and 2000 cal yr BP with a maximum of 12.5% and minimum of 10.2% (mean 11.2%) (Fig. 3). Thereafter the organic matter content decreases and vary between 11.3 and 8.2% (mean 9.9%) from 2000 cal yr BP to about 1960 CE when organic matter content decreases to a mean 8.9% if the high value of the topmost samples (11.4%) is not included. As organic matter is recalculated to accumulation rates and converted to organic carbon accumulation rates the curve shows a very even development over about 3000 years (Fig. 3). There is a low organic carbon accumulation rates from about 3100 cal yr BP to 1950 CE with a mean of 20.1 g $m^{-2}yr^{-1}$ (range of 14.0–28.0). From about 1950 CE a very rapid increase in organic carbon accumulation rates takes place and reached maximum levels of 134.5 g $m^{-2}yr^{-1}$ at 1968 CE. After this peak with a short duration, the values stabilize and display a mean organic carbon accumulation rates of 66.0 g $m^{-2}yr^{-1}$ from the mid 1970s CE to the present, which corresponds to a tripling of organic carbon accumulation rates compared to before the 1950s.

4.3. Stable isotopes

$\delta^{15}N_{OM}$ values ranged 2.6–6.4‰, and those of $\delta^{13}C_{OM}$ ranged between −26.2 and −21.8‰, and the two variables were strongly

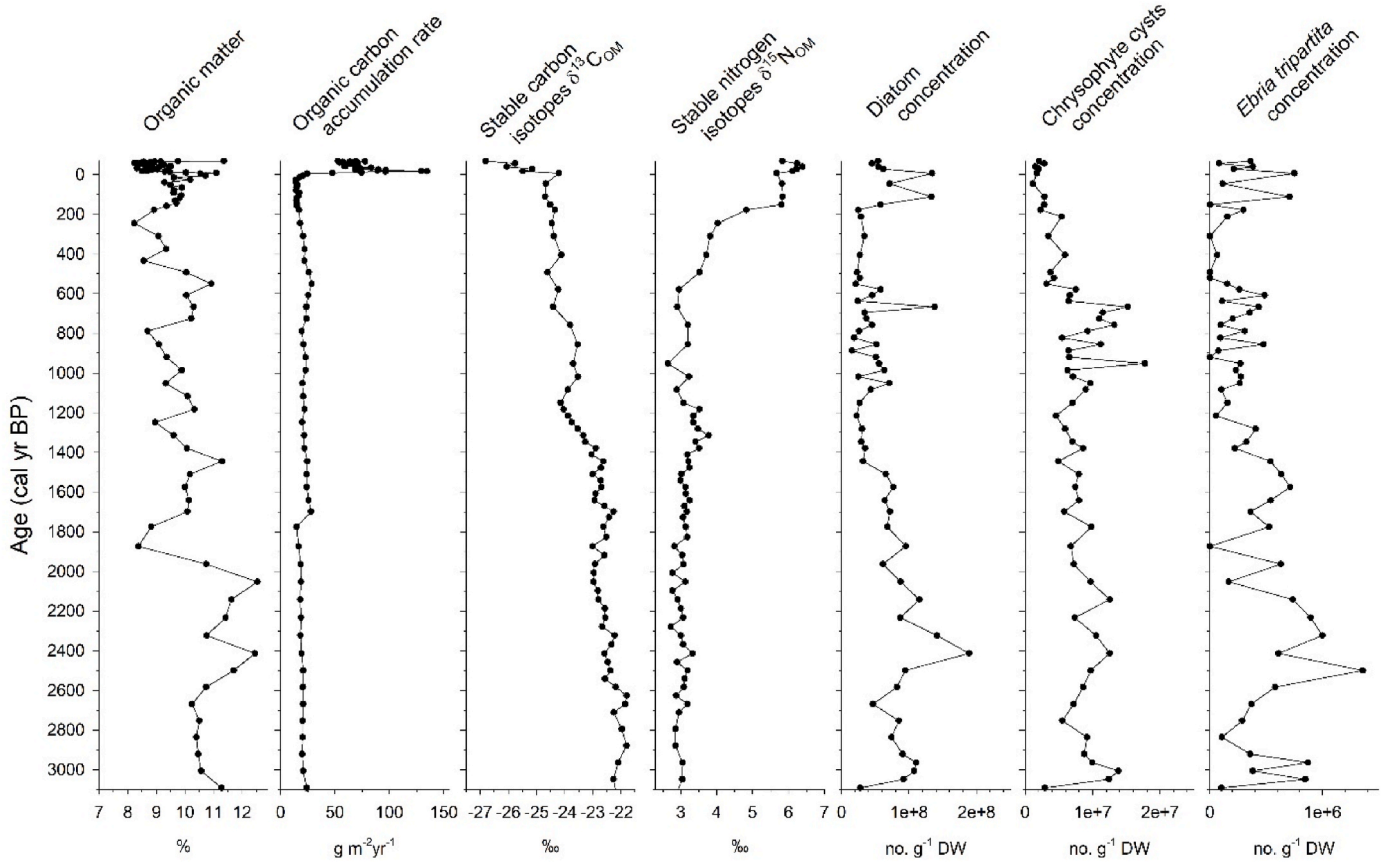

Fig. 3. Gamlebyviken estuary, site EL18-SH01-03: down core profiles in organic matter, organic carbon accumulation rate, stable carbon isotopes $\delta^{13}C_{OM}$, stable nitrogen isotopes $\delta^{15}N_{OM}$ and siliceous microfossils concentrations of diatoms, crysophyte cysts and *Ebria tripartita*.

negatively correlated ($r = -0.79$, $p < 0.001$). Their temporal trends followed, overall, opposite patterns with marked changes observed at *ca.* 1350 cal yr BP, *ca.* 650 cal yr BP and *ca.* 50 cal yr BP (Fig. 3). $\delta^{15}N_{OM}$ and $\delta^{13}C_{OM}$ values remained constant from *ca.* 3000 cal yr BP to *ca.* 1350 cal yr BP with values around 3‰ and −22‰, respectively. The period *ca.* 1350 cal yr BP – *ca.* 650 cal yr BP was characterized by a small decrease in both $\delta^{15}N_{OM}$ and $\delta^{13}C_{OM}$ values until *ca.* 650 cal yr BP when $\delta^{15}N_{OM}$ instead showed a marked increase from 3‰ to 6‰. The most recent period (from *ca.* 50 cal yr BP) was also characterized by drastic changes in sedimentary isotopic composition with a further increase in $\delta^{15}N_{OM}$ values reaching the highest values reported throughout the record (6.4‰) and a marked decrease in $\delta^{13}C_{OM}$ values reaching the lowest values (−26.2‰; Fig. 3).

4.4. Siliceous microfossil concentrations and accumulation rates

Altogether 60 samples were counted for siliceous microfossils, mainly diatoms, but also the siliceous cysts of chrysophytes and the ebridian *Ebria tripartita*. Concentrations (absolute abundance; no. g^{-1} DW) of diatoms, chrysophyte cysts, and *Ebria tripartita* are plotted in Fig. 3. The diatom concentration is highest in the oldest part of the stratigraphy about 3100-1450 cal yr BP with a mean of $8.8*10^7$ valves g^{-1} DW and thereafter decreases to about half until 550 cal yr BP when the minimum concentration of mean $3.1*10^7$ valves g^{-1} DW appears until about 100 cal yr BP (1850 CE) when the concentration increases and show two peaks in the most recent part (mean $7.9*10^7$ valves g^{-1} DW). Chrysophyte cysts show high concentrations (mean $8.7*10^6$ cysts g^{-1} DW) until about 550 cal yr BP and there after a decrease to recent times with a mean of $3.0*10^6$ cysts g^{-1} DW. The concentration of the ebridian *Ebria tripartita* displays a similar development as the diatoms with a clear maximum in the oldest part 3100 to 1450 cal yr BP (mean 5.5*105 skeletons g^{-1} DW), and a minimum between 550 and 150 cal yr BP (1800 CE) with mean of 0.8 skeletons g^{-1} DW.

4.5. Diatom stratigraphy

A total of 293 diatom taxa were identified to the species level. The good degree of preservation of the lightly silicified taxa *Skeletonema marinoi* and *Chaetoceros* vegetative cells indicate that diatoms are not unevenly dissolved, all taxa contribute to the assemblages and are therefore included in the basic sum. The basic sum of counted diatom valves varied between 375 and 1480 depending on the richness of *Chaetoceros* spp. and *S. marinoi*. A diatom species diagram was constructed showing the relative abundances of taxa with more than 3% in any sample, rarefied species richness, and summary graphs of taxa classified into salinity preferences and life forms (Fig. 4). The diatom stratigraphy was divided into four diatom assemblage zones (DAZ) based on cluster analysis (CONISS) and described as follows from the oldest to the youngest:

DAZ 1 (480–415 cm; 3090–2540 cal yr BP) is dominated by a few taxa (mean species richness 39) of planktonic affinity (mean 74.4%). The zone has a maximum occurrence of *Chaetoceros* spp. (mean ca. 53%) which are classified as marine (marine-brackish or brackish-marine; Snoeijs et al. 1993–1998). This dominance is reflected by the most marine conditions inferred across the whole diatom sequence with very low abundance of freshwater and brackish-freshwater taxa (mean sum 8.6%).

DAZ 2 (415–250 cm; 2540–1250 cal yr BP) displays an increase in brackish water taxa (mean ca. 46%) on the expense of marine taxa (mean ca. 29%), but also a doubling of the brackish-freshwater taxa to mean 11.5%. The brackish planktonic taxon *Cyclotella choctawhatcheeana* has maximum abundance and *Skeletonema marinoi* shows high abundance in the lower part and decreases towards the end of the zone. The marine taxon *Thalassiosira eccentrica* has maximum abundance. Species richness has a mean of ca. 48 and there is a visible upward increase of benthic and epiphytic taxa (mean sum ca. 39%).

DAZ 3 (250–72 cm; 1250–130 cal yr BP/700–1820 CE) has a maximum abundance of sea ice taxa, especially *Fragilariopsis cylindrus* but also *Melosira arctica*, visible as two distinct peaks. The lowermost peak (ca. 1210–1085 cal yr BP) has a maximum abundance of 27% and the uppermost peak (ca. 550–210 cal yr BP) has a maximum of 31%. These peaks in sea ice taxa also coincide with the minimum abundance of *Skeletonema marinoi*. The zone also displays a maximum abundance of benthic (including epiphytic taxa, mean 50%). This zone has twice the share of brackish-freshwater taxa (mean 23%) of all the other zones and maximum species richness (mean 53).

DAZ 4 (72–0 cm; 130 to -68 cal yr BP/1820–2018 CE) consists of two clusters 4 A and 4 B of which only the uppermost 4 B (40–0 cm; 1968–2018 CE) is statistically significant. The zone is dominated by planktonic (mean ca. 76%) and brackish taxa (mean ca. 50%) with

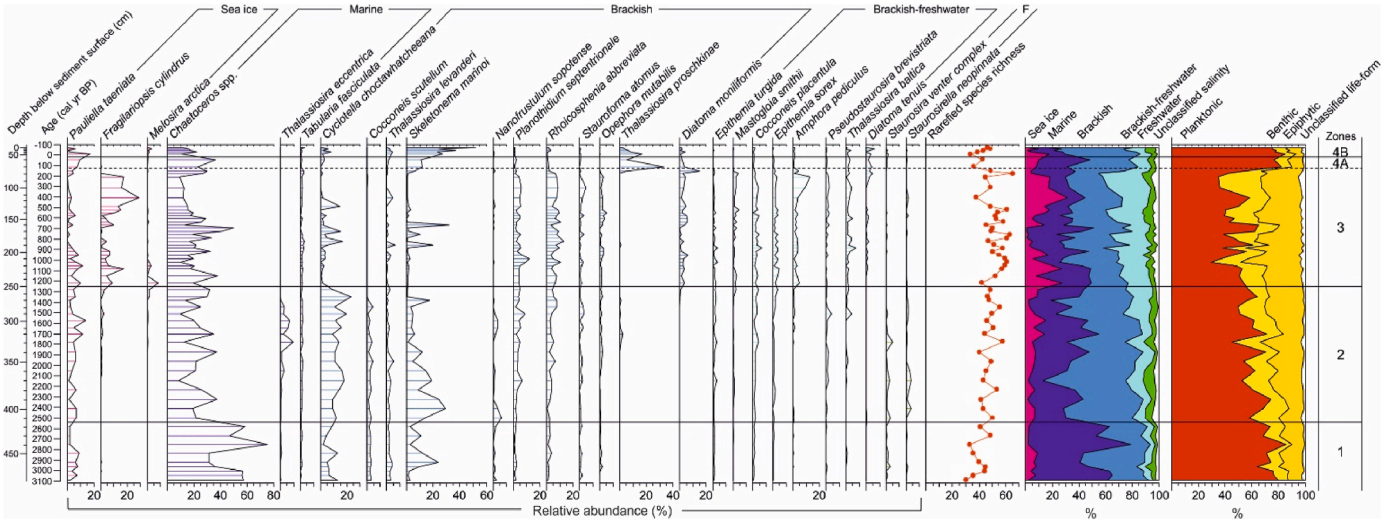

Fig. 4. Gamlebyviken estuary: diatom stratigraphy from site EL18-SH01-03 plotted on a linear age scale showing taxa with a relative abundance of more than 3% in any sample, classified according to salinity affinity and displayed in order of their first appearance. Rarefied species richness (no. of taxa) is plotted to the right. Two cumulative summary graphs show the relative abundance of taxa classified into salinity requirements and life forms, respectively, of all counted diatom taxa. The proportion of benthos classified as epiphytes is indicated by a dark yellow colour. A cluster analysis divided the stratigraphy into four diatom assemblage zones (DAZ1-DAZ4). For a full species list with abbreviations, author names, classification of salinity requirements and life form see Table S3 in Supplementary material.

maximum abundance of *Skeletonema marinoi* and *Thalassiosira proschkinae*. The species richness has decreased to ca. 42 (mean) due to a decrease in benthic taxa and a few dominant planktonic taxa.

4.6. Regional and local vegetation and land use reconstructions

The REVEALS-based regional vegetation cover from the Storsjön pollen record is woodland-dominated. Relatively low at the beginning of the record, the cover of the open land (wetland, grassland, and cropland) gradually increases and reaches its maximum at present (Fig. 5A and 6A).

Between 3080 and 1650 cal yr BP the woodland cover is 77–82%, with deciduous trees having ca. 10% higher cover than coniferous, except for 2250–2050 cal yr BP when it is 14% lower. *Corylus*, *Betula,* and *Alnus* are the most widespread, while *Quercus* and *Tilia* are continuously present but less common. Coniferous woodland consists mainly of *Pinus* with only minor presence of *Picea* (up to 2%). The open land is mainly grassland (15–18%) dominated by Poaceae (9–12%) with continuous occurrence of *Ranunculus acris*-type. *Juniperus* and *Calluna* have up to 2% and 4%, respectively. There are sporadic occurrences of *Artemisia* (ruderal plant). Wetland cover increases from 1 to 5%. Crop cultivation only occurred during 3080–2650 cal yr BP (cropland cover 4%). The landscape generally reflects low anthropogenic impact, mostly through grazing.

The period between 1650 and 1000 cal yr BP shows higher anthropogenic impact with an increase in REVEALS-estimated vegetation openness and a corresponding decrease of the woodland cover to 65–72%. Coniferous and deciduous woodland prevail alternately with ca. 5% difference. The same arboreal taxa remain dominant, but all at a lower percentage than in the previous period. The diversity of herbal taxa increases, and the grassland cover reaches 20–25%, mostly due to an increase in Poaceae and *Rumex acetosa*-type, while *Ranunculus acris*-type becomes much less common. The cover of *Juniperus* and *Calluna* remains similar to the previous period. The occurrence of ruderal plants (*Artemisia* and Amaranthaceae/Chenopodiaceae) stays very low (<1%). Wetland cover reaches its maximum of 11% between 1300 and 1150 cal yr BP, then decreases again to 4% between 1150 and 1000 cal yr BP. Cropland cover increases from 1 to 5%, there is a continuous indication of crop cultivation and the first occurrence of *Secale cereale* between 1150 and 1000 cal yr BP.

Between 1000 cal yr BP and present, the REVEALS-estimated woodland cover decreases from 80 to 60%. Dominance of coniferous woodland (47–59%) is associated with *Picea* establishment after 1000 cal yr BP. Deciduous woodland gradually decreases from 33 to 9% at present, with the decrease of all taxa except for *Fagus* and *Carpinus*. These two taxa have higher values and more continuous occurrence than previously, but also decrease by 250 and 100 cal yr BP, respectively. Grassland cover is 10–13% between 1000 and 700 cal yr BP, gradually increasing to 27% at present. A decrease in Poaceae and *Rumex acetosa*-type after 1000 cal yr BP is followed by a new increase continuing until present. *Juniperus* shows the same trend, while *Calluna* maintains values of 1–3%. *Plantago lanceolata* and ruderal plants *Artemisia* and Amaranthaceae/Chenopodiaceae occur continuously. During this period, pollen of all herbaceous taxa included in the modelling is present, but REVEALS-based estimations of occurrence of some taxa in the landscape are not reliable (*Filipendula*, *Galium*-type, *Potentilla*-type, and Compositae SF Cichorioideae, see explanation to Fig. 5A). Wetland cover is 3–5% except during 250-100 cal yr BP when it reaches 7%. Cropland cover increases gradually from 3 to 9% at present, with lower value of 2% between 400 and 250 cal yr BP.

Local LOVE-reconstructed plant cover based on the Lillsjön pollen profile is woodland-dominated between 3080 and 400 cal yr BP. There is a strong decrease in woodland cover and change to dominance of open-land vegetation from 400 cal yr BP to present (Fig. 5B and 6B).

Between 3080 and 1850 cal yr BP woodland (67–97%) is primarily composed of deciduous trees (56–71%), with only minor part of coniferous woodland (7–25%). *Alnus, Corylus* and *Tilia* dominate, while *Carpinus, Fraxinus, Quercus* and *Ulmus* are continuously present. Coniferous woodland consists predominantly of *Pinus*. Between 2050 and 1850 cal yr BP the woodland cover is the highest in the record (97%), with maximum of deciduous woodland (71%) and increase in coniferous woodland (up to 26%). Open land is predominantly grassland (26–30%), with dominance of Poaceae (up to 22%), apart from 2050 to 1850 cal yr BP, when Poaceae are not part of the pollen record. The only other taxon occurring continuously during this time period is *Filipendula* (up to 3%), while *Galium*-type and *Potentilla*-type are present between 3080 and 1850 cal yr BP (<1%). Wetland cover is ca. 4% between 3080 and 2250 cal yr BP, and decreases to 0–1% afterwards. Cropland cover is only reconstructed between 2650 and 2050 cal yr BP (<1%). The vegetation cover reflects generally low anthropogenic impact through grazing.

Between 1850 and 1150 cal yr BP woodland cover decreases to 53–78% (deciduous woodland 41–70%, coniferous woodland 8–22%). *Corylus* continues to dominate among deciduous trees (12–25%), while presence of *Alnus* and *Tilia* decreases gradually from 17 to ca. 7% and from 12 to 2%, respectively. *Carpinus* and *Quercus* increase to values of ca. 3%. *Fagus, Fraxinus* and *Ulmus* occur continuously. Coniferous woodland is now dominated by *Picea*, which increases gradually from 3 to 16%. Grassland with Poaceae continue to dominate the open-land vegetation (18–38% and 7–23%, respectively). Filipendula occurs continuously but decreases to ca. 1%. *Artemisia* (ruderal) occurs continuously (<1%), while *Galium*-type, *Ranunculus acris*-type, Amaranthaceae/Chenopodiaceae (ruderal) occur almost continuously, as well as *Juniperus* and *Calluna* (up to 6% and 4%, respectively). Wetland cover is ca. 7% in the middle of the period but is lower/absent at its beginning and the end. There is a continuous record of cropland (ca. 2%) except for 1450-1300 cal yr BP, when it reaches 9%. This period is characterized by increase in anthropogenic impact with higher grazing activity and increase in crop cultivation.

The period between 1150 and 400 cal yr BP is distinguished by the new increase in woodland cover (69–83%) due to the increase in *Picea* (from 29 to 43–55%) that continues to dominate the coniferous woodland. The cover of the deciduous woodland decreases to 28–36%. The same taxa remain dominant, but most (apart form *Quercus* and *Corylus*) do not occur continuously, and all have lower values. There is a notable increase in *Salix* (up to 4%), while *Betula* occurs continuously for the first time in the record (2–7%). Grassland cover decreases gradually from 29 to 12% and Poaceae from 20 to 7%. Apart from Poaceae, only *Filipendula* occurs continuously (0.5–2%), while *Ranunculus acris*-type has the highest values in the record (up to 2.5%). Wetland cover is 5% in the middle of this period, but only up to 2% or absent otherwise. Crop cultivation occurs during the whole period, but cropland cover only reaches 2%. Especially the middle of this period is characterized by low anthropogenic activity.

Between 400 cal yr BP and present the woodland cover, interchangingly dominated by deciduous and coniferous woodland, decreases strongly and is the lowest in the record (19%) between 250 and 100 cal yr BP. *Alnus, Fagus, Quercus* and *Betula* are the only taxa with continuous occurrence, but their values are decreasing towards present. *Carpinus, Tilia* and *Corylus* are not present or have very low values. *Picea* remains dominant in the coniferous woodland. Cover of grassland increases strongly and is the highest in the record (46%) between 250 and 100 cal yr BP primarily due to increase in Poaceae (up to 29%), but also *Rumex acetosa*-type (up to 4%) and Compositae SF Cichorioidae (up to 9%). *Filipendula* and Amaranthaceae/Chenopodiaceae are continuously

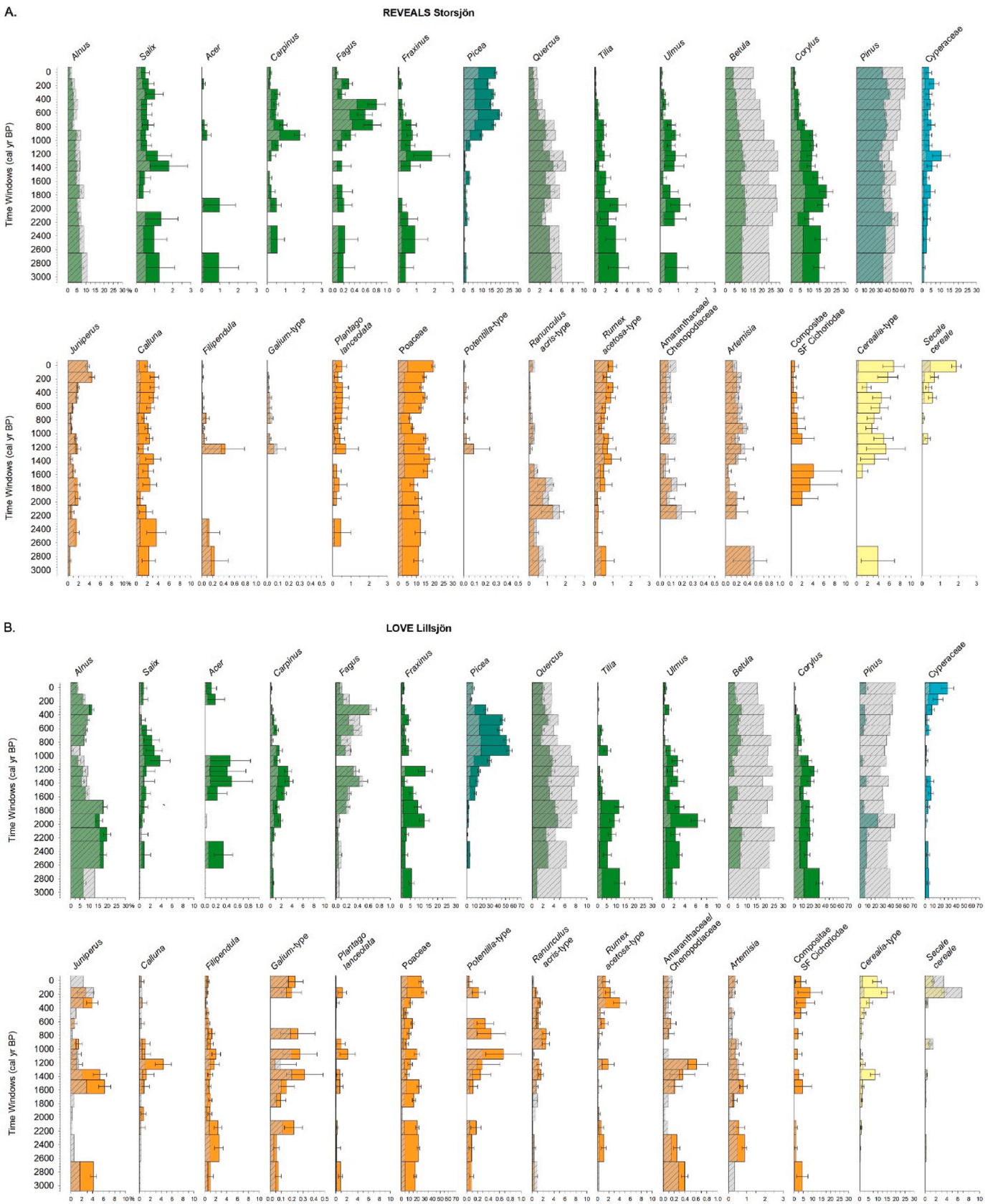

Fig. 5. Gamlebyviken estuary: modelled land cover data from lake Storsjön using REVEALS and lake Lillsjön using LOVE for 16 time-windows. REVEALS estimates of regional (A.) and LOVE estimates of local (B.) plant cover in % cover with their standard error (colored with bars) and pollen % (grey) for 28 taxa. Note: When standard error ⩾ REVEALS/LOVE estimate, the estimates of plant cover are not reliable. Green: deciduous woodland; emerald green: coniferous woodland; turquoise: wetland; orange: grassland; yellow: cropland.

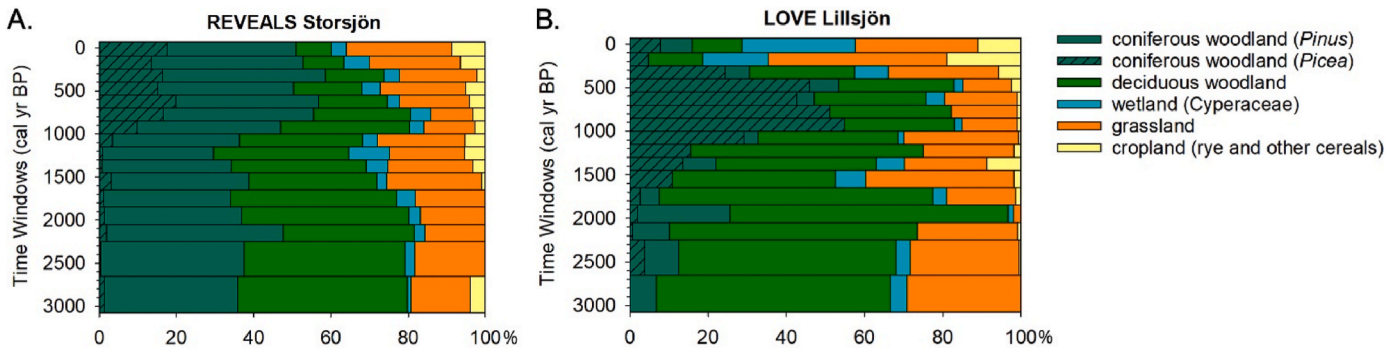

Fig. 6. Gamlebyviken estuary: summary graphs showing taxa used in the REVEALS (A.) and LOVE (B.) modelling grouped into five land cover types: coniferous woodland (*Pinus* and *Picea*), deciduous woodland, wetland (Cyperaceae), grassland (including *Juniperus*) and cropland (cereals) (modified after Mazier et al., 2015).

present (<1%). Wetland cover increases gradually towards present and is the highest (29%) between 100 cal yr BP and present. There is a strong increase in cropland cover with maximum of 18% simultaneous to the largest grassland cover.

4.7. Statistics

The plot of the PCA analysis with the explanatory variables regressed on to the ordination shows that deciduous woodland, $\delta^{13}C_{OM}$, Age BP, and Temperature are higher towards the upper right and lower towards the lower left (Fig. 7). Wetland and coniferous woodland follow the same diagonal but are higher in the lower left. Cropland, grassland, and $\delta^{15}N_{OM}$ form a cluster of regression directions of their own. All regressions are significant at $P = 0.001$. The older samples cluster together in the upper right corner showing that there were smaller changes in the diatom composition then. The youngest samples are found in the center bottom and the rest of the more recent samples are quite spread out showing faster differentiation in more recent years.

In the RDA analysis (Table 2) we look for the size of the unique effects on diatom composition for each variable when the effect of the others is removed. Cropland and grassland represent land use in this analysis. The strongest effect is from $\delta^{13}C_{OM}$, then from the two land use types cropland and grassland. AgeBP and $\delta^{15}N_{OM}$ have lower but still significant effects while the effect of Temperature is not significant. The pattern is different from the regression of each variable on the PCA ordination which are included in Table 2 for comparison, e.g. Temperature has a large r^2 value in the regression on the PCA but when the unique explanatory power is distributed among the variables little is left.

To evaluate differences in time we combined the two younger diatom cluster zones, younger than 1250 cal yr BP, and compared with the combined two older cluster zones >1250 cal yr BP. We partitioned the variation between AgeBP, Temperature, $\delta^{15}N_{OM}$ and Land use (grassland and cropland together). The variation partitioning (Fig. 8) shows that the variables explain more variation in the younger part. The contribution of Temperature is larger in the older part 7 and 3%, respectively, and the contribution of $\delta^{15}N_{OM}$ and Land use is larger in the younger part, together 26% compared to 15%. The contribution of AgeBP is similar, at 7%, in both time periods and therefore not plotted in Fig. 8.

The correlation of diatom species to the environmental variables is shown in Table S4 and Fig. 7B, and suggests that a group of diatom

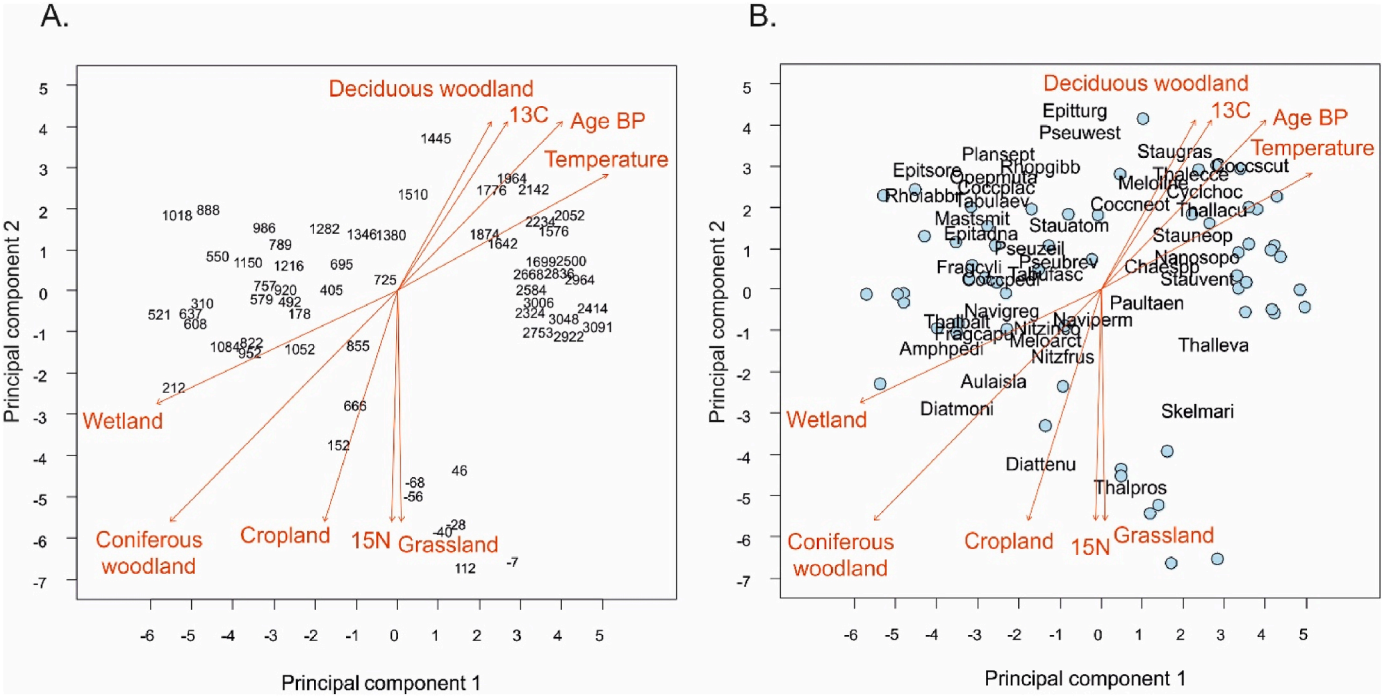

Fig. 7. Gamlebyviken estuary: Principal component analysis (PCA) for an overview of the association of the explanatory variables with the diatom assemblage composition. Each explanatory variable was regressed onto the ordination to show the direction and evaluate the significance of their association. A. Sample scores (ages cal yr BP), B. Diatom species scores (abbreviation of diatom taxa is found in Table S3, Supplementary material).

Table 2
Results from an RDA analysis where each variable is tested for significance when the effect of all others is removed. For comparison the results from the regression of the variables on the PCA are included.

Variable	Df Variance	F	P	PCA r^2	PCA P
AgeBP	1 0.0056	2.34	0.038 *	0.71	0.001 ***
Temperature	1 0.0041	1.74	0.086.	0.73	0.001 ***
13C	1 0.0134	5.58	0.001 ***	0.76	0.001 ***
15 N	1 0.0050	2.13	0.042 *	0.65	0.001 ***
Grassland	1 0.0075	3.15	0.004 **	0.37	0.001 ***
Cropland	1 0.0090	3.75	0.002 **	0.71	0.001 ***
Residual	53 0.1268				

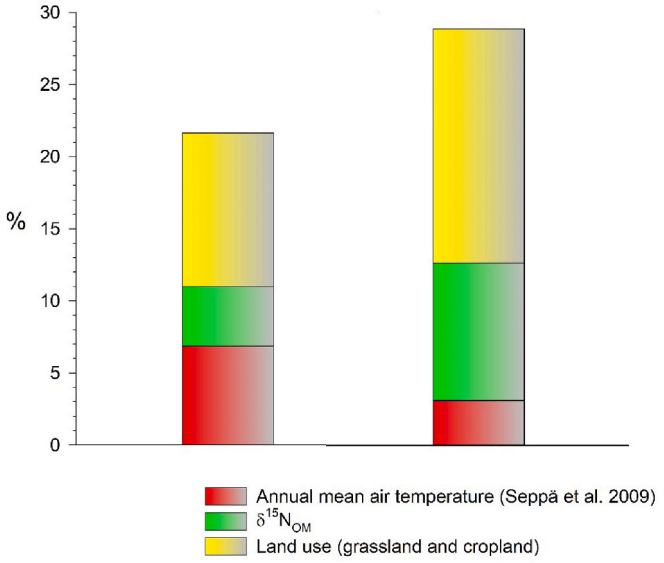

Fig. 8. Gamlebyviken estuary: variation partitioning to separate the impacts of the factors land use changes (stable nitrogen isotopes $\delta^{15}N_{OM}$ and grassland and cropland) and climate (annual mean air temperature) on the diatom abundance data. The data set was divided into two parts: old, >1250 cal yr BP (left) and young, <1250 cal yr BP (right), both containing two diatom clusters.

species is associated with AgeBP, Temperature, $\delta^{13}C_{OM}$ and deciduous woodland and another group with $\delta^{15}N_{OM}$, coniferous woodland, grassland and croplands and to some extent wetlands. Strong positive correlations (>0.5) for croplands are found for *Aulacoseira islandica* (Aulaisla), *Diatoma moniliformis* (Diatmoni), *Diatoma tenuis* (Diattenu) and *Thalassiosira proschkinae* (Thalpros), and strong negative association were found for *Cocconeis scutellum* (Coccscut), *Staurosirella guenter-grassii* (Staugras) and *Thalassiosira eccentrica* (Thalecce). Grasslands and $\delta^{15}N_{OM}$ are strongly positively correlated with *Diatoma tenuis* (Diattenu) and *Thalassiosira proschkinae* (Thalpros) (Table S4, Supplementary material).

5. Discussion

5.1. Hypoxia and salinity

In the open Baltic Sea, the observed increase in hypoxia in contemporary times is attributed to eutrophication, primarily stemming from heightened nutrient inputs originating from terrestrial and atmospheric sources (Meier et al., 2019). Furthermore, this trend has been exacerbated over recent decades by deoxygenation resulting from escalating temperatures (Carstensen and Conley, 2019). Within the coastal zone, the occurrence of hypoxia exhibits variability and is dependent upon various factors. These factors encompass the quantity of organic material derived from primary production, which consumes oxygen during decomposition, as well as physical parameters such as the presence of enclosed areas characterized by limited water exchange and stable stratification, influenced by temperature or salinity gradients. Coastal hypoxia occurrences are classified as episodic, seasonal, or persistent manifestations (Conley et al., 2011). In our case study area in Gamlebyviken, the lithology of the sediment core indicates that hypoxia has persisted in the estuary for the past 3000 years. This condition has been attributed to the limited water exchange between the enclosed basin and the open Baltic Sea, resulting in stable stratification coupled with high primary productivity.

By utilizing knowledge of shoreline displacement and constructing a paleogeographic map depicting the configuration of water-land in our study area 3000 years ago when the water level was approximately 11.3 m higher than today (Katransiotis et al., 2024), it becomes evident that water exchange at our study site, with only an archipelago of islands

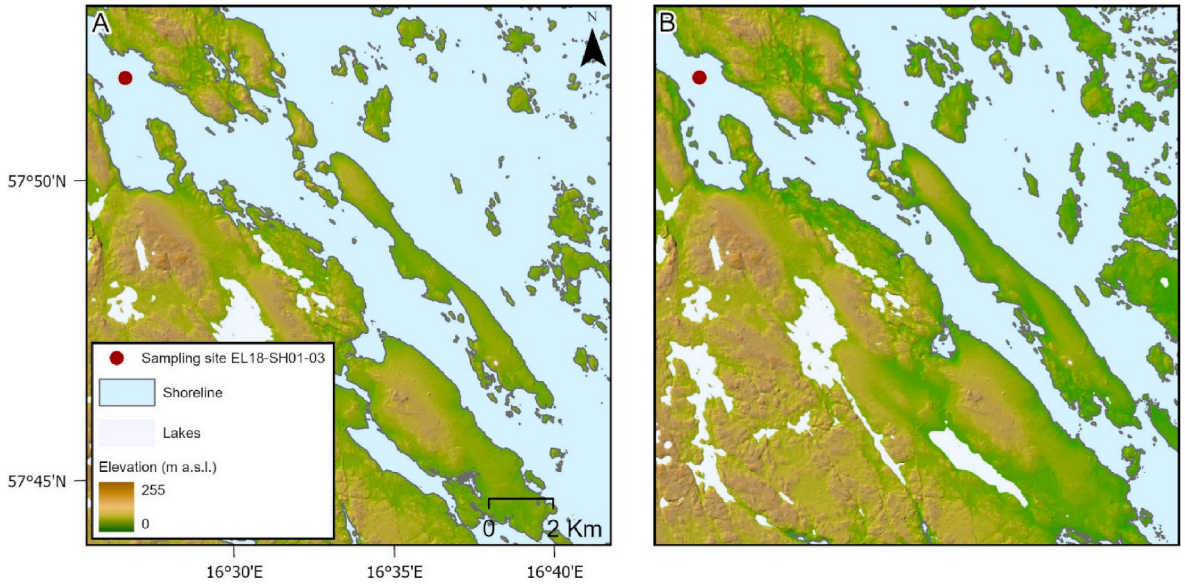

Fig. 9. Paleogeographic maps illustrate the land-sea configuration of a specific area over time. A. At 3000 cal yr BP, the sea level was +11.3 m, resulting in a more open marine environment and enhanced water circulation, consequently raising salinity at the sampling site. B. By 1300 cal yr BP, the sea level had decreased to +3 m, shaping the current layout of the Gamlebyviken estuary, distinguished by a narrow inlet located where the town of Västervik presently stands (see Fig. 1B).

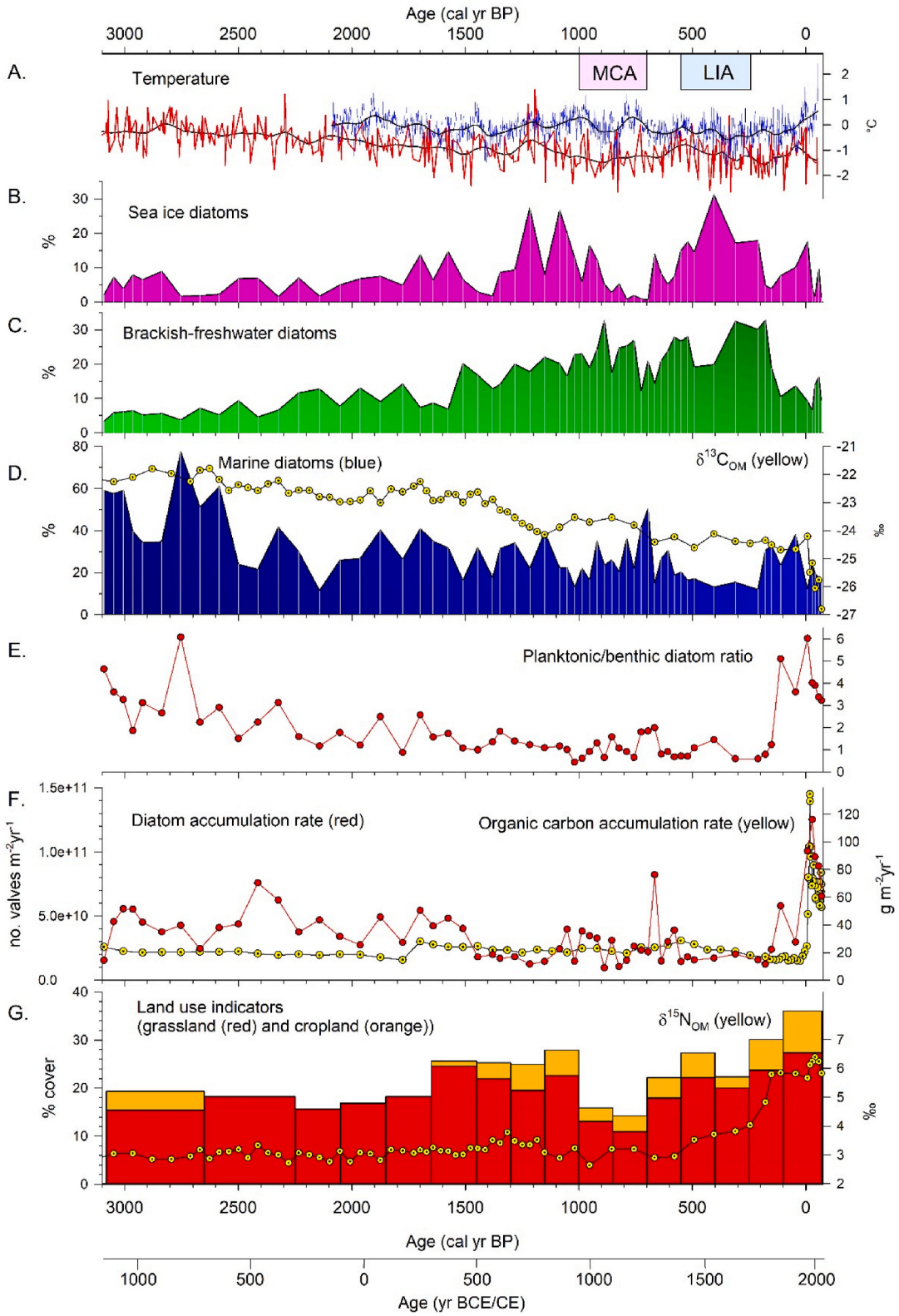

Fig. 10. Summary graph to display the major environmental change in the Gamlebyviken area on linear age axis (cal yr BP or BCE/CE years), and the climatic events discussed in the text, the Medieval Climate Anomaly (MCA) and the Little Ice Age (LIA) are marked. A. Annual temperature anomaly (red curve) reconstructed from North European pollen records (Seppä et al., 2009) used in the statistics in the present paper, compared to European summer temperatures (blue curve) reconstructed from tree-rings (Luterbacher et al., 2016). Both curves smoothed with LOESS span of 0.05. B-D. Relative percentages of diatom assemblages divided into sea ice taxa (B), brackish-freshwater taxa (C) and marine taxa (D) and stable carbon isotopes (yellow line) used as proxy for the carbon source, marine – terrigenous origin, respectively. E. Planktonic/benthic (including epiphytes) diatom ratio. F. Diatom accumulation rate (red line, as no. of valves per square m and year) and organic carbon accumulation rate (yellow line, as g carbon per square m and year). G. Land use indicators (grassland (red bars) and cropland (orange bars)) reconstructed from Storsjön (Fig. 6A) and stable nitrogen isotopes (yellow line).

separating it from the open Baltic Sea, was more effective at that time (Fig. 9A). This configuration likely resulted in the more marine conditions recorded, as evidenced by the maximum in marine diatom assemblage dominated by *Chaetoceros* spp. (Fig. 4, DAZ1; Fig. 10D). Gradually, the land uplift in our study area, as depicted in the paleogeographic map from 1300 cal yr BP (+3 m sea level; Fig. 9B), transformed the archipelago into a peninsula, shaping the current configuration of the Gamlebyviken estuary with a sole water exchange occurring through the narrow inlet at Västervik. This transformation is clearly manifested in the increase in brackish-freshwater diatom taxa at the expense of marine taxa, coupled with a decline in $\delta^{13}C_{OM}$ values, indicating reduced marine primary production and a more sheltered environment with slightly increased terrestrial input (Fig. 10).

5.2. Changes in the Baltic sea coastal zone before 1000 cal yr BP (Bronze Age and Iron Age)

During the Bronze Age the regional vegetation cover in our study area was predominantly characterized by deciduous woodland (Fig. 6). Early human influence on the landscape, confirmed by archaeological mapping (Vinogradova et al., 2024), may have involved land clearance for animal husbandry, potentially serving as a nutrient source to coastal areas during this period, evidenced by the high planktonic diatom production recorded (Fig. 10D; Fig. 10 F). The diatom assemblage was dominated by marine genera, particularly *Chaetoceros* spp., known to thrive in nutrient-rich waters with upwelling conditions (Armbrecht et al., 2014). The abundance of spring-blooming diatoms such as *Chaetoceros* spp., *Skeletonema marinoi*, and summer-blooming *Cyclotella choctawhatcheeana*, alongside high stable carbon isotope values (Fig. 10D), signifies a nutrient-rich and highly productive coastal environment. This high primary production might also have promoted elevated concentrations of the heterotrophic protist *Ebria tripartita* since it is known to feed on diatoms (Hargraves, 2002). However, despite the high diatom accumulation rate observed between 3000 and 2000 cal yr BP, there was no discernible impact on the organic carbon accumulation rate (Fig. 10F). Additionally, the PCA plot indicates minimal differentiation between samples in the older part of the stratigraphy (Fig. 7). These findings suggest that despite extensive local and some regional land clearance, there was little to no discernible impact on the Baltic Sea coastal zone environment in our study area.

The period exhibiting the greatest potential impact of both regional and local land use on the coastal zone, except for the most recent era, extends from 1650 to 1000 cal yr BP (300–950 CE), corresponding to the Late Iron Age, a period with high grassland and increasing cropland cover at the regional scale (Fig. 10G). However, this influence is not discernible in the paleoecological proxies derived from the estuary. A low diatom accumulation rate characterized by sparse planktonic taxa (low planktonic/benthic diatom ratio; Fig. 10E) and a low organic carbon accumulation rate are documented and only a slight rise in $\delta^{15}N_{OM}$ is indicative of the cropland expansion seen in the vegetation reconstructions (see Fig. 10G). The influence of land use in the coastal zone during this time frame may potentially be tempered by the colder climatic conditions prevailing (Luterbacher et al., 2016), as evidenced by peaks in sea ice diatom taxa (Fig. 10B).

5.3. Changes in the Baltic sea coastal zone after 1000 cal yr BP (medieval times, Little Ice Age, and modern times)

In contrast to other parts of Sweden, medieval times in our study area witnessed regional and local afforestation with its maximum recorded ca. 1000-700 cal yr BP, characterized by a notable increase in coniferous woodland cover due to the expansion of spruce (*Picea*). It is also a period of strong decrease in land use, with the lowest regional grassland cover in the record (Figs. 5A and 6A). We propose this period as experiencing the least impact of nutrient discharge to coastal waters in our study area, a notion corroborated by paleoecological proxies revealing low organic carbon- and diatom accumulation rates, and a diminished planktonic/benthic diatom ratio (Fig. 10). These findings align with the conclusions drawn by Andrén et al. (2020) who attribute climate as the primary driver of drier and more marine conditions with intensified stratification in the open Baltic Sea during that period. Model projections further support this view, indicating a reduction in precipitation during positive Atlantic multidecadal variability states, prevalent during the Medieval Climate Anomaly, which would have resulted in arid conditions and heightened salinity levels in the Baltic Sea (Börgel et al., 2022). Some variations in the diatom assemblages may plausibly be linked to slightly elevated temperatures during the Medieval Climate Anomaly, evidenced by a decrease in sea ice taxa, alongside peaks in *Skeletonema marinoi, Cyclotella choctawhatcheeana*, and *Chaetoceros* spp. (Fig. 4), despite the low and stable organic carbon accumulation rates (Fig. 10).

Species richness was relatively high throughout the stratigraphy, twice the number found in a open Baltic Sea setting (Andrén et al., 2020), with a maximum during the colder and less productive Little Ice Age when benthic taxa increased on the expense of the planktonic (Fig. 10E).The Little Ice Age (550-250 cal yr BP/1400–1700 CE, Mann et al., 2009), when compared to the Medieval Climate Anomaly, is distinctly reflected in our diatom proxy data, with a marked increase in sea ice diatoms, low planktonic/benthic diatom ratio, reduced marine taxa, and elevated brackish-freshwater taxa (Fig. 10), indicating cooler winter temperatures and wetter conditions, consistent with findings in other studies (e.g., Luoto and Nevalainen, 2018). However, this colder period did not mitigate land use in the proximity of the Gamlebyviken and local evidence indicates an expansion of cultivated cropland starting from 400 cal yr BP (Vinogradova et al., 2024). Regionally, the general trend of increasing landscape openness and crop cultivation from 700 cal yr BP is interrupted by a twofold decrease in cropland cover and slight decrease in grassland 400–250 cal yr BP, not reflected in the local reconstructions. Concurrent with increased land use (both cropland and grassland), the $\delta^{15}N_{OM}$ signal commenced its ascent from a low level during the Little Ice Age and peaked around 1800 CE. This rise in $\delta^{15}N_{OM}$ aligns with stable nitrogen isotope trends from other coastal regions in the Baltic Sea (Voss et al., 2000), albeit occurring earlier (ca. 200 cal yr BP/1750 CE) in our study area, similar to findings in another Swedish coastal site (Norbäck-Ivarsson et al., 2019), attributable to deforestation, alongside the last century of eutrophication.

The most significant changes in the Gamlebyviken occurred from about 100 cal yr BP/1850 CE up to present times, with maximum regional cover of grassland and cropland (ca. 35%) at the expense of deciduous woodland and major changes indicative of a highly eutrophic environment recorded in the coastal zone. These changes are visible as maxima in the stable nitrogen isotopes, carbon- and diatom accumulation rates, as well as maximum planktonic/benthic diatom ratio and diatom species indicative of high nutrient conditions, in particular, *Thalassiosira proschkinae* and *Diatoma tenuis* (Fig. 10; Table S4, Supplementary material). The same diatom taxa indicating high nutrient levels are recorded from Bråviken on the Swedish east coast (Norbäck Ivarsson et al., 2019). However, the primary similarity between our record and observed diatom responses to eutrophication in other studies is the significant shift to planktonic species dominance, recorded along the Swedish east coast (Norbäck Ivarsson et al., 2019), the German coast (Andrén, 1999; Andrén et al., 1999), and the Finnish coast (Weckström, 2006). These studies document the onset of human-induced eutrophication, reflecting the local environmental histories of the sites, spanning from 1800 to 1940 CE. Similar trends in stable nitrogen isotopes and carbon accumulation rates are found in other studies of the Baltic Sea proper's coastal areas, such as Finland (Jokinen et al., 2018) and the Swedish east coast near the present study site (Ning et al., 2018), although the absolute values are higher in Gamlebyviken. The carbon isotope values began to be depleted around 1968 CE, with decreasing values continuing to the present (Fig. 3). This change coincides with maxima in both organic carbon and diatom accumulation rates (Fig. 10F). If the stable carbon isotope signal had reflected high primary

production in the estuary, an enrichment would have been expected (Savage et al., 2010). We interpret the depleted carbon isotope values as a response to increased discharge from terrestrial sources (Lamb et al., 2006), possibly due to intensified land use (Fig. 10G). Organic carbon accumulation rates peaked in 1968 CE at approximately 134 g C/m^2 yr^{-1} before subsequently declining to the present-day values of 53, mirroring a similar trend observed in diatom accumulation rates. Furthermore, the rate of organic carbon accumulation in Gamlebyviken is in pair with well-documented shallow coastal carbon sinks (e.g. seagrass meadows with a global average organic carbon accumulation rate of 138 g C/m^2 yr^{-1}; Mcleod et al., 2011) and shows that deeper accumulation bottoms in the coastal Baltic Sea are worth exploring for their ability to mitigate climate change. Most of the studies on coastal carbon sinks in the Baltic Sea region have been conducted in vegetated habitats (i.e. salt marshes, seagrass meadows and macroalgae belts), which generally display lower accumulation rates in comparison to this study (ranging from 5 to 253 g C/m^2 yr^{-1}; Krause-Jensen et al., 2022) and with deeper unvegetated sediment bottoms being overlooked.

5.4. Climate versus human impact

It has been demonstrated that during the Medieval Climate Anomaly in the open Baltic Sea, stratification, both thermal and salinity-related, emerged as the primary climatic mechanism influencing diatoms, rather than the elevated temperatures alone (Andrén et al., 2020). It is noteworthy that climate variability encompasses more than just heightened temperatures; it also entails increased rates of weathering and changes in freshwater discharge, which affect the transport of nutrients from land into the basin. This complex interplay complicates the explanation of the effects of climate variability from those attributable to changes in land use.

Variation partitioning shows that 26% of the variance in the diatom assemblages during the last 1250 years is associated with land use changes. The variables grassland, cropland, and stable nitrogen isotopes are accordingly strong predictors of environmental change in the Baltic coastal zone as reflected by the diatoms (Fig. 8). The total variance explained increases in the younger part (last 1250 years), especially stable nitrogen isotopes that more than double at the expense of variance explained by temperature. In the more pristine environment (>1250 cal yr BP) the temperature played an important role in affecting the diatom assemblages (Fig. 8). This may be a result of the selection of climate proxy in our statistical analyses, where we apply reconstructed annual mean temperature anomalies derived from North European pollen records (Seppä et al., 2009). While this model spans the 3000-year timeframe under scrutiny in our study, it fails to capture significant climatic events such as the Roman Warm Period (2200-1550 cal yr BP/250 BCE–400 CE, Campbell et al., 1998) and the Medieval Climate Anomaly, a deficiency highlighted when contrasting it with the European summer temperature reconstruction based on tree-rings (Fig. 10A; Luterbacher et al., 2016). Furthermore, the discernible temperature rise observed over the past 150 years due to global climate change is absent in the Seppä et al. (2009) dataset, potentially influencing interpretations regarding the climatic impact on diatom populations during the same time period. Over the past 50 years, we have recorded a notable peak in the abundance of the spring-blooming marine diatom *Skeletonema marinoi*. This increase is likely more closely associated with rising temperatures than with eutrophication, which is supported by the taxon's high abundance during other periods characterized by elevated temperatures, such as the Bronze Age and the Medieval Climate Anomaly, and its minimal abundance during the Little Ice Age (Fig. 4).

Ditching and clearance of wetlands and draining of lakes to expand arable land was intensive in Sweden between 1850 and 1950 CE (Hoffmann et al., 2000). These wetlands and lake ecosystems as well as the coastal filter play a crucial role in capturing and storing nutrients within organic sediments (Asmala et al., 2017; Carstensen et al., 2020). Our findings indicate that the study area has experienced prolonged human influence, characterized by multiple instances of land clearance dating back to the Bronze Age and continuing thereafter. However, it was not until about 1800 CE (150 cal yr BP) that the effects of intensified land use began to manifest in the coastal zone, evidenced by increased $\delta^{15}N_{OM}$ levels and heightened planktonic diatom production. This correlates to increased leaching of nitrogen due to the intensive exploitation of lakes and wetlands which caused an extensive drop in nitrogen retention (Hoffmann et al., 2000). The initiation of modern agriculture post-World War II with widespread use of artificial fertilizers, triggered eutrophication in the open Baltic Sea (Carstensen and Conley, 2019). This development is distinctly evident in our dataset, marked by peaks in organic carbon and diatom accumulation rates around 1970 CE, followed by a subsequent decline to the present day, mirroring the trend in nutrient loads originating from land (Gustafsson et al., 2012) with maximum leaching of nitrogen in the mid-1970s (Hoffmann et al., 2000).

6. Conclusions

- The Gamlebyviken area reveals a coastal environment characterized by elevated primary production and restricted water exchange with the open Baltic Sea, resulting in stable stratification and hypoxia over the past 3000 years.
- Approximately 3000 years ago, when the sea level was approximately 11 m higher than now, our study indicates a more efficient water exchange between our site and the open Baltic Sea, facilitating more pronounced marine conditions. The subsequent decline in marine conditions within Gamlebyviken from approximately 2500 years ago can be attributed to ongoing shoreline displacement, culminating in the present fjord-like estuarine configuration with a narrow inlet.
- Our findings suggest sustained human influence in the study area, characterized by recurrent land clearance activities dating back to the Bronze Age and persisting thereafter.
- During medieval times in our study area, there was a regional afforestation phase between 1000 and 500 cal yr BP (950–1450 CE), marked by the expansion of spruce at the expense of deciduous trees and related to a decrease in land use 1000–700 cal yr BP. This time period experienced the least impact of nutrient discharge to the Baltic Sea coastal waters.
- The influence of the Little Ice Age is evident in our diatom proxy data, indicating cooler winter temperatures and increased precipitation. Despite these colder climatic conditions, there was no noticeable reduction in land use activities. On the contrary, local evidence suggests a significant expansion of cultivated cropland around 400 cal yr BP.
- The effects of intensified land use began to manifest in the coastal zone around 1800 CE, as evidenced by increased $\delta^{15}N_{OM}$ levels and heightened planktonic diatom production.
- The most pronounced impact on the coastal Baltic Sea in the case study area occurred around 1950–1970 CE, with significant changes indicative of a highly eutrophic environment, as evidenced by organic carbon accumulation rates reaching approximately 134 g C/m^2 yr^{-1} in 1968 CE, before subsequently declining to present-day values of 53 g C/m^2 yr^{-1}, mirroring a similar trend observed in diatom accumulation rates.
- Deep unvegetated accumulation bottoms in the coastal Baltic Sea serve as carbon sinks and are worth exploring for their potential in mitigating climate change.
- Grassland, cropland, and stable nitrogen isotopes emerge as robust predictors of environmental change in the Baltic Sea coastal zone, as reflected by diatom assemblages. Stable nitrogen isotopes exhibit a strong association with grassland and cropland and can serve as a reliable proxy for land use.

- Both climate and land use represent crucial variables for elucidating environmental changes in the Baltic Sea coastal zone over time; however, eutrophic conditions were not observed in the Gamlebyviken estuary during medieval times.

CRediT authorship contribution statement

Elinor Andrén: Conceptualization, Project administration, Writing – original draft, Formal analysis, Visualization, Investigation, Funding acquisition, Data curation. **Olena Vinogradova:** Writing – original draft, Formal analysis, Visualization, Investigation, Data curation. **Mikael Lönn:** Writing – original draft, Methodology, Formal analysis, Visualization. **Simon Belle:** Writing – original draft, Formal analysis. **Martin Dahl:** Writing – original draft, Formal analysis, Visualization. **Veronica Palm:** Writing – review & editing, Investigation. **Christos Katrantsiotis:** Writing – review & editing, Resources, Data curation. **Anne Birgitte Nielsen:** Writing – review & editing, Resources, Data curation. **Martin Jakobsson:** Writing – review & editing, Investigation. **Johan Rönnby:** Writing – review & editing, Investigation, Funding acquisition. **Thomas Andrén:** Conceptualization, Writing – original draft, Formal analysis, Visualization, Investigation, Funding acquisition.

Funding

This research was made possible through funding from the Foundation for Baltic and East European Studies, grant number 3146-3.1.1-2017, awarded to EA. Funding was provided to MD by the Foundation for Baltic and East European studies (grant number: 21-PD2-0002).

Declaration of competing interest

The authors declare that they have no known competing financial interests or personal relationships that could have appeared to influence the work reported in this paper.

Acknowledgements

We express our gratitude to the captain and crew of R/V Electra af Askö, Stockholm University, for providing excellent fieldwork conditions in the Gamlebyviken estuary. We extend our appreciation to Anders Amelin (sadly deceased) for conducting the LOI measurements at Södertörn University. Special thanks are also due to Professor Marie-José Gaillard, Linnaeus University for contributing to the interpretation of the vegetation history and to Professor Heikki Seppä, University of Helsinki, for sharing the pollen-inferred temperature data. Finally, we acknowledge the comments and suggestions provided by the editor professor Patrick Rioual, and the two anonymous referees.

Appendix A. Supplementary data

Supplementary data to this article can be found online at https://doi.org/10.1016/j.quascirev.2024.109058.

Data availability

The siliceous microfossil data related to this article can be found at https://doi.org/10.17043/andren-2024-gamlebyviken-microfossil-1, and the geochemistry data at https://doi.org/10.17043/andren-2024-gamlebyviken-geochemistry-1, an open-source online data repository hosted by the Bolin Centre Database (https://bolin.su.se/data/).

References

Ahti, T., Hamet-Ahti, L., Jalas, J., 1968. Vegetation zones and their sections in northwestern Europe. Ann. Bot. Fenn. 5, 169–211.

Åkesson, C., 2013. Pollen analytical and landscape reconstruction study at Lake Storsjön, southern Sweden, over the last 2000 years. Master's Thesis No. 360, Department of Geology. Dissertations in Geology at Lund University, Lund.

Åkesson, C., Nielsen, A.B., Broström, A., Persson, T., Gaillard, M.-J., Berglund, B.E., 2015. From landscape description to quantification: a new generation of reconstructions provides new perspectives on Holocene regional landscapes of SE Sweden. Holocene 25, 178–193. https://doi.org/10.1177/0959683614556552.

Andrén, E., van Wirdum, F., Norbäck Ivarsson, L., Lönn, M., Moros, M., Andrén, T., 2020. Medieval versus recent environmental conditions in the Baltic Proper, what was different a thousand years ago? Palaeogeogr. Palaeoclimatol. Palaeoecol. 555, 109878. https://doi.org/10.1016/j.palaeo.2020.109878.

Andrén, E., 1999. Changes in the composition of the diatom flora during the last century indicate increased eutrophication of the oder estuary, south-western Baltic Sea. Estuar. Coast Shelf Sci. 48, 665–676. https://doi.org/10.1006/ecss.1999.0480.

Andrén, E., Andrén, T., Kunzendorf, H., 2000a. Holocene history of the Baltic Sea as a background for assessing records of human impact in the sediments of the Gotland Basin. Holocene 10, 687–702. https://doi.org/10.1191/09596830094944.

Andrén, E., Andrén, T., Sohlenius, G., 2000b. The Holocene history of the southwestern Baltic Sea as reflected in a sediment core from the Bornholm Basin. Boreas 29, 233–250. https://doi.org/10.1111/j.1502-3885.2000.tb00981.x.

Andrén, E., Shimmield, G., Brand, T., 1999. Changes in the environment during the last centuries on the basis of siliceous microfossil records from the southwestern Baltic Sea. Holocene 9, 25–38. https://doi.org/10.1191/095968399676523977.

Andrén, T., Björck, S., Andrén, E., Conley, D., Zillén, L., Anjar, J., 2011. The development of the Baltic Sea basin during the last 130 ka. The Baltic Sea basin. In: Harff, J., Björck, S., Hoth, P. (Eds.), Central and Eastern European Development Studies (CEEDES). Springer-Verlag, Berlin Heidelberg, pp. 75–97.

Appleby, P.G., 2001. Chronostratigraphic techniques in recent sediments. In: M Last, W., Smol, J.P. (Eds.), Tracking Environmental Change Using Lake Sediments, Vol 1: Basin Analysis, Coring and Chronological Techniques. Kluwer Academic Publishers, Dordrecht, pp. 171–204.

Armbrecht, L.H., Roughan, M., Rossi, V., Schaeffer, A., Davies, P.L., Waite, A.M., Armand, L.K., 2014. Phytoplankton composition under contrasting oceanographic conditions: upwelling and downwelling (Eastern Australia). Continent. Shelf Res. 75, 54–67. https://doi.org/10.1016/j.csr.2013.11.024.

Asmala, E., Carstensen, J., Conley, D.J., Slomp, C.P., Stadmark, J., Voss, M., 2017. Efficiency of the coastal filter: nitrogen and phosphorus removal in the Baltic Sea. Limnol. Oceanogr. 62, S222–S238. https://doi.org/10.1002/lno.10644.

Battarbee, R.W., Kneen, M.J., 1982. The use of electronically counted microspheres in absolute diatom analysis. Limnol. Oceanogr. 27, 184–188. https://doi.org/10.4319/lo.1982.27.1.0184.

Battarbee, R.W., 1986. Diatom analysis. In: Berglund, B.E. (Ed.), Handbook of Holocene Palaeoecology and Palaeohydrology. Johan Wiley & Sons Ltd., Chichester, pp. 527–570.

Berglund, B.E. (Ed.), 1991. The Cultural Landscape during 6000 Years in Southern Sweden: the Ystad Project. Ecological Bulletins 41. Munksgaard International Booksellers and Publishers, Copenhagen, p. 495.

Bianchi, T.S., Engelhaupt, E., Westman, P., Andrén, T., Rolff, C., Elmgren, R., 2000. Cyanobacterial blooms in the Baltic Sea: natural or human-induced? Limnol. Oceanogr. 45, 716–726. https://doi.org/10.4319/lo.2000.45.3.0716.

Birks, H.J.B., Line, J.M., 1992. The use of rarefaction analysis for estimating palynological richness from quaternary pollen-analytical data. Holocene 2, 1–10. https://doi.org/10.1177/095968369200200101.

Blaauw, M., Christen, J., Aquino Lopez, M., 2022. Rbacon: age-depth modelling using bayesian statistics. R package version 2.5.8. https://CRAN.R-project.org/package=rbacon.

Blaauw, M., Christen, A., 2011. Flexible paleoclimate age-depth models using an autoregressive gamma process. Bayesian Analysis6 (3), 457–474. https://doi.org/10.1214/11-BA618.

Börgel, F., Meier, H.E.M., Gröger, M., Rhein, M., Dutheil, C., Kaiser, J.M., 2022. Atlantic multidecadal variability and the implications for North European precipitation. Environ. Res. Lett. 17, 044040. https://doi.org/10.1088/1748-9326/ac5ca1.

Breitburg, D., Levin, L.A., Oschlies, A., Grégoire, M., Chavez, F.P., Conley, D.J., Garçon, V., Gilbert, D., Gutiérrez, D., Isensee, K., Jacinto, G.S., Limburg, K.E., Montes, I., Naqvi, S.W.A., Pitcher, G.C., Rabalais, N.N., Roman, M.R., Rose, K.A., Seibel, B.A., Telszewski, M., Yasuhara, M., Zhang, J., 2018. Declining oxygen in the global ocean and coastal waters. Science 359, eaam7240. https://doi.org/10.1126/science.aam7240.

Carstensen, J., Conley, D.J., 2019. Baltic Sea hypoxia takes many shapes and sizes. Limnol. Oceanogr. 28 (4), 125–129. https://doi.org/10.1002/lob.10350.

Carstensen, J., Conley, D.J., Almroth-Rosell, E., Asmala, E., Bonsdorff, E., Fleming-Lehtinen, V., Gustafsson, B.G., Gustafsson, C., Heiskanen, A.-S., Janas, U., Norkko, A., Slomp, C., Villnäs, A., Voss, M., Zilius, M., 2020. Factors regulating the coastal filter in the Baltic Sea. Ambio 49, 1194–1210. https://doi.org/10.1007/s13280-019-01282-y.

Clarke, A.L., Weckström, K., Conley, D.J., Anderson, N.J., Adser, F., Andrén, E., de Jonge, V.N., Ellegaard, M., Juggins, S., Kauppila, P., Korhola, A., Reuss, N., Telford, R.J., Vaalgamaa, S., 2006. Long-term trends in eutrophication and nutrients in the coastal zone. Limnol. Oceanogr. 51, 385–397. https://doi.org/10.4319/lo.2006.51.1_part_2.0385.

Conley, D.J., Humborg, C., Rahm, L., Savchuk, O.P., Wulff, F., 2002. Hypoxia in the Baltic Sea and basin-scale changes in phosphorus biogeochemistry. Environ. Sci. Technol. 36 (24), 5315–5320. https://doi.org/10.1021/es025763w.

Conley, D.J., Carstensen, J., Aigars, J., Axe, P., Bonsdorff, E., Eremina, T., Haahti, B.-M., Humborg, C., Jonsson, P., Kotta, J., Lännegren, C., Larsson, U., Maximov, A., Medina, M.R., Lysiak-Pastuszak, E., Remeikaite-Nikiene, N., Walve, J., Wilhelms, S.,

Zillén, L., 2011. Hypoxia is increasing in the coastal zone of the Baltic Sea. Environ. Sci. Technol. 45, 6777–6783. https://doi.org/10.1021/es201212r.
Dean, W.E., 1974. Determination of carbonate and organic matter in calcareous sediments and sedimentary rocks by loss on ignition: comparison with other methods. J. Sediment. Petrol. 44, 242–248.
Emanuelsson, U., 2009. The rural landscapes of Europe. How Man Has Shaped European Nature. The Swedish Research Council Formas, p. 383.
Eniro På sjön, 2022. https://pasjon.eniro.se/.
Grimm, E.C., 1987. CONISS: a FORTRAN 77 program for stratigraphically constrained cluster analysis by the method of incremental sum of squares. Comput. Geosci. 13, 13–35. https://doi.org/10.1016/0098-3004(87)90022-7.
Gustafsson, B., Schenk, F., Blenckner, T., Eilola, K., Meier, H.E.M., Müller-Karulis, B., Neumann, T., Ruoho-Airola, T., Savchuk, O.P., Zorita, E., 2012. Reconstructing the development of Baltic Sea eutrophication 1850–2006. Ambio 41, 534–548. https://doi.org/10.1007/s13280-012-0318-x.
Guiry, M.D., Guiry, G.M., 2024. AlgaeBase. World-wide Electronic Publication. University of Galway. https://www.algaebase.org. (Accessed 27 October 2024).
Hargraves, P.E., 2002. The ebridian flagellates *Ebria* and *Hermesinum*. Plankton Biol. Ecol. 49, 9–16.
Hasle, G.R., Syvertsen, E.E., 1997. Chapter 2 - marine diatoms. In: Tomas, C.R. (Ed.), Identifying Marine Phytoplankton. Academic Press, San Diego, pp. 5–385. https://doi.org/10.1016/B978-012693018-4/50004-5.
Heaton, T.J., Köhler, P., Butzin, M., et al., 2020. Marine20—the marine radiocarbon age calibration curve (0–55,000 cal BP). Radiocarbon 62 (4), 779–820. https://doi.org/10.1017/RDC.2020.68.
HELCOM, 2007. Climate change in the Baltic Sea area – HELCOM thematic assessment in 2007. Baltic Sea Environment Proceedings No. 111, 49.
Hoffmann, M., Johnsson, H., Gustafson, A., Grimvall, A., 2000. Leaching of nitrogen in Swedish agriculture — a historical perspective. Agric. Ecosyst. Environ. 80, 277–290. https://doi.org/10.1016/S0167-8809(00)00154-7.
Jokinen, S.A., Virtasalo, J.J., Jilbert, T., Kaiser, J., Dellwig, O., Arz, H.W., Hänninen, J., Arppe, L., Collander, M., Saarinen, T., 2018. A 1500-year multiproxy record of coastal hypoxia from the northern Baltic Sea indicates unprecedented deoxygenation over the 20th century. Biogeosciences 15, 3975–4001. https://doi.org/10.5194/bg-15-3975-2018.
Jonsson, P., Carman, R., Wulff, F., 1990. Laminated sediments in the Baltic Sea–a tool for evaluating nutrient mass balances. Ambio 19, 152–158.
Jonsson, P., 2003. Skärgårdens bottnar. Naturvårdsverket Rapport 5212, p. 112 pp (In Swedish with English summary).
Juggins, S., 2015. Rioja: analysis of quaternary science data. Available at: https://cran.r-project.org/web/packages/rioja/index.html.
Kabel, K., Moros, M., Porsche, C., Neumann, T., Adolphi, F., Andersen, T.J., Siegel, H., Gerth, M., Leipe, T., Jansen, E., Damsté, J.S.S., 2012. Impact of climate change on the Baltic Sea ecosystem over the past 1,000 years. Nat. Clim. Change 2, 871–874. https://doi.org/10.1038/nclimate1595.
Krammer, K., Lange-Bertalot, H., 1986-1991. In: Ettl, H., Gärtner, J.G., Gerloff, J., Heynig, H., Mollenhauer, D. (Eds.), Süsswasserflora von Mitteleuropa Bd 2. Stuttgart: Fischer. T. 1, Naviculaceae (1986), T. 2, Bacillariaceae, Epithemiaceae, Surirellaceae (1988), T. 3, Centrales, Fragilariaceae, Eunotiaceae (1991) and T. 4, Achnanthaceae (1991).
Katrantsiotis, C., Vinogradova, O., Dahl, M., Palm, V., Rönnby, J., Gaillard, M.J., Andrén, T., Andrén, E., 2024. Holocene shoreline displacement, land-cover change and human settlement distribution at the southeast coast of Sweden. J. Quat. Sci. https://doi.org/10.1002/jqs.3666 (in press).
Krause-Jensen, D., Gundersen, H., Björk, M., Gullström, M., Dahl, M., Asplund, M.E., et al., 2022. Nordic blue carbon ecosystems: status and outlook. Front. Mar. Sci. 9, 847544. https://doi.org/10.3389/fmars.2022.847544.
Kursa, M.B., Rudnicki, W.R., 2010. Feature selection with the boruta package. J. Stat. Software 36 (11), 1–13. URL. http://www.jstatsoft.org/v36/i11/.
Lagerås, P., 2016. Environment, Society and the Black Death: an Interdisciplinary Approach to the Late-Medieval Crisis in Sweden. Oxbow Books, Oxford, p. 208.
Lamb, A.L., Wilson, G.P., Leng, M.J., 2006. A review of coastal palaeoclimate and relative sea-level reconstructions using $\delta^{13}C$ and C/N ratios in organic material. Earth Sci. Rev. 75, 29–57. https://doi.org/10.1016/j.earscirev.2005.10.003.
Leppäranta, M., Myrberg, K., 2009. Physical Oceanography of the Baltic Sea. Springer, Berlin Heidelberg, p. 378.
Lougheed, B.C., Filipsson, H.L., Snowball, I., 2013. Large spatial variations in coastal 14C reservoir age - a case study from the Baltic Sea. Clim. Past 9, 1015–1028. https://doi.org/10.5194/cp-9-1015-2013.
Luoto, T.P., Nevalainen, L., 2018. Temperature-precipitation relationship of the Common Era in northern europe. Theor. Appl. Climatol. 132, 933–938. https://doi.org/10.1007/s00704-017-2139-0.
Luterbacher, J., Werner, J.P., Smerdon, J.E., Fernández-Donado, L., González-Rouco, F. J., Barriopedro, D., Ljungqvist, F.C., Büntgen, U., Zorita, E., Wagner, S., Esper, J., McCarroll, D., Toreti, A., Frank, D., Jungclaus, J.H., Barriendos, M., Bertolin, C., Bothe, O., Brázdil, R., Camuffo, D., Dobrovolný, P., Gagen, M., García-Bustamante, E., Ge, Q., Gómez-Navarro, J.J., Guiot, J., Hao, Z., Hegerl, G.C., Holmgren, K., Klimenko, V.V., Martín-Chivelet, J., Pfister, C., Roberts, N., Schindler, A., Schurer, A., Solomina, O., von Gunten, L., Wahl, E., Wanner, H., Wetter, O., Xoplaki, E., Yuan, N., Zanchettin, D., Zhang, H., Zerefos, C., 2016. European summer temperatures since Roman times. Environ. Res. Lett. 11, 024001. https://doi.org/10.1088/1748-9326/11/2/024001.
Mann, M.E., Zhang, Z., Rutherford, S., Bradley, R.S., Hughes, M.K., Shindell, D., Ammann, C., Faluvegi, G., Ni, F., 2009. Global signatures and dynamical origins of the little ice age and medieval climate anomaly. Science 326, 1256–1260. https://doi.org/10.1126/science.1177303.
Mazier, F., Broström, A., Bragée, P., et al., 2015. Two hundred years of land-use change in the South Swedish Uplands: comparison of historical map-based estimates with a pollen-based reconstruction using the landscape reconstruction algorithm. Veg. Hist. Archaeobotany 24 (5), 555–570. https://doi.org/10.1007/s00334-015-0516-0.
Mcleod, E., Chmura, G.L., Bouillon, S., Salm, R., Björk, M., Duarte, C.M., et al., 2011. A blueprint for blue carbon: toward an improved understanding of the role of vegetated coastal habitats in sequestering CO2. Front. Ecol. Environ. 9 (10), 552–560. https://doi.org/10.1890/110004.
Meier, H.E.M., Eilola, K., Almroth-Rosell, E., Schimanke, S., Kniebusch, M., Höglund, A., Pemberton, P., Liu, Y., Väli, G., Saraiva, S., 2019. Disentangling the impact of nutrient load and climate changes on Baltic Sea hypoxia and eutrophication since 1850. Clim. Dynam. 53, 1145–1166. https://doi.org/10.1007/s00382-018-4296-y.
Meier, H.E.M., Kniebusch, M., Dieterich, C., Gröger, M., Zorita, E., Elmgren, R., Myrberg, K., Ahola, M., Bartosova, A., Bonsdorff, E., Börgel, F., Capell, R., Carlén, I., Carlund, T., Carstensen, J., Christensen, O.B., Dierschke, V., Frauen, C., Frederiksen, M., Gaget, E., Galatius, A., Haapala, J.J., Halkka, A., Hugelius, G., Hünicke, B., Jaagus, J., Jüssi, M., Käyhkö, J., Kirchner, N., Kjellström, E., Kulinski, K., Lehmann, A., Lindström, G., May, W., Miller, P., Mohrholz, V., Müller-Karulis, B., Pavón-Jordán, D., Quante, M., Reckermann, M., Rutgersson, A., Savchuk, O.P., Stendel, M., Tuomi, L., Viitasalo, M., Weisse, R., Zhang, W., 2022. Climate Change in the Baltic Sea Region: A Summary. Earth System Dynamics 13, 457–593. https://doi.org/10.5194/esd-13-457-2022.
Meiners, K., Fehling, J., Granskog, M.A., Spindler, M., 2002. Abundance, biomass and composition of biota in Baltic sea ice and underlying water (March 2000). Polar Biol. 25, 761–770. https://doi.org/10.1007/s00300-002-0403-x.
Morell, 2011. Agriculture in industrial society 1870-1945. In: Myrdal, Janken, Morell, Mats (Eds.), The Agrarian History of sweden : from 4000 BC to AD 2000. Nordic academic press, Lund, pp. 165–213.
Munsell Soil Color Book, 2009. Munsell Soil Color Charts, 2009 Year Revised. Grand Rapids US.
Myrdal, J., 2011. Farming and feudalism 1000–1700. In: Myrdal, J., Morell, M. (Eds.), The Agrarian History of Sweden: from 4000 BC to AD 2000. Nordic Academic Press, Lund, pp. 72–117. https://doi.org/10.1016/j.ancene.2018.02.003.
Ning, W., Nielsen, A.B., Norbäck Ivarsson, L., Jilbert, T., Åkesson, C.M., Slomp, C.P., Andrén, E., Broström, A., Filipsson, H.L., 2018. Anthropogenic and climatic impacts on a coastal environment in the Baltic Sea over the last 1000 years. Anthropocene 21, 66–79. https://doi.org/10.1016/j.ancene.2018.02.003.
Norbäck Ivarsson, L., Andrén, T., Moros, M., Andersen, T.J., Lönn, M., Andrén, E., 2019. Baltic Sea coastal eutrophication in a thousand years perspective. Front. Environ. Sci. 7, 88. https://doi.org/10.3389/fenvs.2019.00088.
Oksanen, J., Simpson, G.L., Blanchet, F.G., Kindt, R., Legendre, P., Minchin, P.R., O'Hara, R.B., Solymos, P., Stevens, M.H.H., Szoecs, E., Wagner, H., Barbour, M., Bedward, M., Bolker, B., Borcard, D., Carvalho, G., Chirico, M., De Caceres, M., Durand, S., Weedon, J., 2022. Vegan: Community Ecology Package, 2.vols. 6–2. R Foundation for Statistical Computing, Vienna (Austria). Available at: https://cran.r-project.org/web/packages/vegan/index.html.
Pedersen, E.A., Widgren, M., 2011. Agriculture in Sweden: 800 BC-ad 1000. In: Myrdal, Janken, Morell, Mats (Eds.), The Agrarian History of Sweden: from 4000 BC to AD 2000. Nordic academic press, Lund, pp. 46–71.
R Core Team, 2022. R: A Language and Environment for Statistical Computing. R Foundation for Statistical Computing, Vienna, Austria. URL. https://www.R-project.org/.
Reimer, P., Austin, W., Bard, E., Bayliss, A., Blackwell, P., Bronk Ramsey, C., Talamo, S., 2020. The IntCal20 Northern Hemisphere Radiocarbon Age Calibration Curve (0–55 cal kBP). Radiocarbon 62 (4), 725–757. https://doi.org/10.1017/RDC.2020.41.
Savage, C., Leavitt, P.R., Elmgren, R., 2010. Effects of land use, urbanization, and climate variability on coastal eutrophication in the Baltic Sea. Limnol. Oceanogr. 55 (3), 1033–1046. https://doi.org/10.4319/lo.2010.55.3.1033.
Schimanke, S., Meier, H.E.M., Kjellström, E., Strandberg, G., Hordoir, R., 2012. The climate in the Baltic Sea region during the last millennium simulated with a regional climate model. Clim. Past 8, 1419–1433. https://doi.org/10.5194/cp-8-1419-2012.
Seppä, H., Bjune, A.E., Telford, R.J., Birks, H.J.B., Veski, S., 2009. Last nine-thousand years of temperature variability in Northern Europe. Clim. Past 5, 523–535. https://doi.org/10.5194/cp-5-523-2009.
SGU The Geological Survey of Sweden, 2022. Soil types 1:25 000-1:100 000; Bedrock 1:1 million. Available at: https://www.sgu.se/en/products/maps/map-viewer/jordkartvisare/soil-types-125-000-1100-000/ https://www.sgu.se/en/products/maps/map-viewer/bedrock-map-viewers/bedrock-11-million/.
Sjörs, H., 1999. The background: geology, climate and zonation. In: Rydin, H., Snoeijs, P., Diekmann, M. (Eds.), Swedish Plant Geography, 1–248, Acta Phytogeographica Suecia, vol. 84. Uppsala.
SMHI Swedish Meteorological and Hydrological Institute, 2022. Swedish climate. Available at: https://www.smhi.se/data/meteorologi/kartor/.
Snoeijs, P., et al., 1993-1998. In: Snoeijs, P., Balashova, N. (Eds.). Intercalibration and Distribution of Diatom Species in the Baltic Sea, vol. 5 Vol. 1-5 Opulus press, Uppsala Vol 1 (1993). Snoeijs, P. ed., Vol 2 (1994). Snoeijs, P., and Vilbaste, S. eds., Vol 3 (1995). Snoeijs, P., and Potapova, M. eds., Vol 4 (1996). Snoeijs, P., and Kasperovičienė, J. eds., Vol. 5 (1998).
Snoeijs-Leijonmalm, P., Andrén, E., 2017. Why is the Baltic Sea so special to live in? In: Snoeijs-Leijonmalm, P., Schubert, H., Radziejewska, T. (Eds.), Biological Oceanography of the Baltic Sea. Springer, Dordrecht., pp. 23–84. https://doi.org/10.1007/978-94-007-0668-2_2
Sohlenius, G., Sternbeck, J., Andrén, E., Westman, P., 1996. Holocene history of the Baltic Sea as recorded in a sediment core from the gotland deep. Mar. Geol. 134, 183–201. https://doi.org/10.1016/0025-3227(96)00047-3.
Stuiver, M., Reimer, P.J., 1993. Calib rev. 8. Radiocarbon 35, 215–230.

Sugita, S., 2007a. Theory of quantitative reconstruction of vegetation I: pollen from large sites REVEALS regional vegetation composition. Holocene 17 (2), 229–241. https://doi.org/10.1177/0959683607075837.

Sugita, S., 2007b. Theory of quantitative reconstruction of vegetation II: all you need is LOVE. Holocene 17 (2), 243–257. https://doi.org/10.1177/0959683607075838.

Svantesson, S.-I., 1999. Beskrivning till jordartskarta 7G Västervik SO/7H loftahammar SV. SGU. Serie Ae 124, 109. In Swedish.

Thomas, D.N., Kaartokallio, H., Tedesco, L., Majaneva, M., Piiparinen, J., Eronen-Rasimus, E., Rintala, J.-M., Kuosa, H., Blomster, J., Vainio, J., Granskog, M.A., 2017. Life associated with Baltic Sea ice. In: Snoeijs-Leijonmalm, P., Schubert, H., Radziejewska, T. (Eds.), Biological Oceanography of the Baltic Sea. Springer, Dordrecht., pp. 333–357. https://doi.org/10.1007/978-94-007-0668-2_9

Vahtera, E., Conley, D.J., Gustafsson, B.G., Kuosa, H., Pitkänen, H., Savchuk, O.P., Tamminen, T., Viitasalo, M., Voss, M., Wasmund, N., Wulff, F., 2007. Internal ecosystem feedbacks enhance nitrogen-fixing cyanobacteria blooms and complicate management in the Baltic Sea. Ambio 36 (2/3), 186–194. http://www.jstor.org/stable/4315813.

Vinogradova, O., Gaillard, M.-J., Andrén, E., Palm, V., Rönnby, J., Dahl, M., Almgren, E., Karlsson, J., Nielsen, A.B., Åkesson, C., Andrén, T., 2024. 3000 Years of past regional and local land-use and land-cover change in the southeastern Swedish coastal area: early human-induced increases in landscape openness as a potential nutrient source to the Baltic Sea coastal waters. Holocene 34 (1), 56–73. https://doi.org/10.1177/09596836231200433.

VISS, 2022. Vatteninformationssystem Sverige. https://viss.lansstyrelsen.se/.

Voss, M., Larsen, B., Leivuori, M., Vallius, H., 2000. Stable isotope signals of eutrophication in Baltic Sea sediments. J. Mar. Syst. 25, 287–298. https://doi.org/10.1016/S0924-7963(00)00022-1.

Weckström, K., 2006. Assessing recent eutrophication in coastal waters of the gulf of Finland (Baltic Sea) using subfossil diatoms. J. Paleolimnol. 35, 571–592. https://doi.org/10.1007/s10933-005-5264-1.

Welinder, S., 2011. Early farming households 3900-800 BC. In: Myrdal, J., Morell, M. (Eds.), The Agrarian History of Sweden from 4000 BC to AD 2000. Nordic Academic press, p. 336.

Winterhalter, B., Flodén, T., Ignatius, H., Axberg, S., Niemistö, L., 1981. Geology of the Baltic Sea. In: Voipio, A. (Ed.), The Baltic Sea. Elsevier Oceanography Series 30, pp. 1–121.

Witkowski, A., Lange-Bertalot, H., Metzeltin, D., 2000. Diatom flora of marine coasts. Iconogr. Diatomol. 7 (Ruggell), 950. Gantner.

Zillén, L., Conley, D.J., Andrén, T., Andrén, E., Björck, S., 2008. Past occurrences of hypoxia in the Baltic Sea and the role of climate variability, environmental change and human impact. Earth Science Review 91, 77–92. https://doi.org/10.1016/j.earscirev.2008.